國 立 交 通 大 學

機械工程研究所
博 士 論 文

六邊形離心調速器的旋轉機械之渾沌控制
及渾沌同步

Chaos Control and Chaos Synchronization for a Rotational Machine with a Hexagonal Centrifugal Governor

研究生：李青一

指導教授：戈正銘　教授

中華民國九十三年六月

六邊形離心調速器的旋轉機械之渾沌控制及渾沌同步

研 究 生：李青一　　　　　　　　　　　指導教授：戈正銘教授

國立交通大學機械工程研究所

摘要

　　本篇論文研究一帶六邊形調速器之旋轉機械的渾沌動力行為，自治、非自治及時滯系統均予以討論。由李亞普諾夫直接法可求得自治系統平衡點的穩定條件。應用一些數值分析，如相圖、功率譜法、龐加萊映射法、及李亞普諾夫指數可觀察到週期解與渾沌運動。參數變化對系統的影響可以由分歧圖及參數圖表現出來。除此之外，利用一些控制方法來有效地控制渾沌現象。最後，對於系統的渾沌反控制與渾沌同步，也提供了控制器設計的一些方法。

Chaos Control and Chaos Synchronization for a Rotational Machine with a Hexagonal Centrifugal Governor

Student　Ching-I Lee　　　　　　　　Advisor　Zheng-Ming Ge

Institute of Mechanical Engineering

National Chiao Tung University

ABSTRACT

The chaotic dynamics of the rotational machine with a hexagonal centrifugal governor are studied in this thesis. Autonomous, nonautonomous and time-delay systems are discussed. The Lyapunov direct method is applied to obtain conditions of stability of the equilibrium points of autonomous system. By applying numerical results, phase diagrams, power spectrum, Poincaré maps, and Lyapunov exponents are presented to observe periodic and chaotic motions. The effect of the parameter changes in the system can be found in the bifurcation and parametric diagrams. Besides, several methods are used to control chaos effectively. Finally, some different procedures for the design of the controller are proposed for anticontrol and synchronization of chaos of the governor system.

誌　謝

CONTENTS

LIST OF FIGURES

Chapter 1

Introduction

During the past one and half decades, a large number of studies have shown that chaotic phenomena are observed in many physical systems that possess non-linearity. It was also reported that the chaotic motion occurred in many nonlinear control system [1-4].

In nature, most of physical systems are nonlinear and can be described by the nonlinear equations of motion. If the nonlinear term can be ignored, it is possible to linearize and easily solve it by the already known methods. The linearization process is reasonable, whereas for some nonlinear systems the simplification is inadequate and inaccure. Hence the researches of nonlinear systems spread quickly today. For the nonlinear system, the study of the types of periodic solutions, the effects to the solutions caused by different parameters and initial conditions, the stability analysis of the solutions, consist of the major tasks. Besides, a substantial understanding of the complicated phenomena arised from nonlinearity is also what we are interested in. The central characteristics are that a process like randomization happens in the deterministic system and small differences in the initial conditions produce very great ones in the final phenomena. The irregular and unpredictable motions of many nonlinear systems have been labeled 'chaotic'. In the end of nineteen century Poncaré first pointed out some important concepts of chaos theory like homoclinic, bifurcation, ...etc. Lorenz researched the strange

changes in the atmosphere which is the first example to study chaos in 1963. A large number of studies on the chaotic behavior have been reached up to now.

A characteristic property of chaotic dynamics is the sensitive dependence on initial condition. Different initial conditions may cause entirely different trajectories for the system. However, Pecora and Carroll [5] showed that synchronization can be achieved for the chaotic systems. This interest phenomenon plays a significant role in the chaotic dynamics of communication signals and may be applied to the real-time recovery of signals that have been masked in a strange attractor and thus to encode communication. Other applications of synchronization of chaos also have expectative potential [6-10].

Sometimes, chaos is not only useful but actually important. For example, chaos is desirable in many applications of liquid mixing while the required energy is minimized. For this purpose, making a non-chaotic dynamical system chaotic is called "anticontrol of chaos". This implies that the regular behaviors will be destroyed and replaced by chaotic behavior. In the real world, chaotic behavior is important. Examples include liquid mixing, humam heartbeat regulations, resonance prevention in mechanical systems and secure communication[11].

In previous researches, most of them are concentrated to several well-known systems, such as Lorenz system, Rössler system and Chua's circuits system, etc. In this thesis, an autonomous hexagonal centrifugal governor system is studied. The centrifugal governor is a device that automatically controls the speed of an engine and prevents the damage caused by sudden change of load torque. It plays an important role in many rotational machines such as diesel engine, steam engine and so on. When an engine

system is subjected to external disturbances, the speed of the engine will vary. In order to diminish the change of engine speed, and avoid the chaotic motion emerging in the operational process of the engine, in this thesis the regular and chaotic dynamics of a rotational machine with centrifugal governor is studied in detail. Furthermore, controlling chaos, synchronization and anticontrol of chaos of the governor system are also studied.

A lot of modern techniques are used in analyzing the deterministic nonlinear system behavior. Both analytical and computational methods are employed to obtain the characteristics of the nonlinear systems. In Chapter 2, the governing equations of motion will be formulated then the stability of the fixed points of the autonomous system are studied by the Lyapunov direct method.

In Chapter 3, many numerical techniques are studied for analyzing the nonlinear system behavior. A variety of the periodic solutions and the phenomena of the chaotic motion can be presented in the phase diagrams, Poincaré maps and power spectrum. The effect of the parameters changed in the system can be found in the bifurcation and parametric diagrams. Further, chaotic motion can be detected by using Lyapunov exponents and Lyapunov dimensions. In order to improve the performance of a dynamic system or to avoid the chaotic phenomena, we must control a chaotic motion to a periodic motion that is beneficial for working with a particular condition. It is thus of great practical importance to develop suitable control methods. Recently much interest has been focused on this type of problem - controlling chaos[4,6,12]. For this purpose, one uses various methods for controlling chaos. The addition of constant motor torque, the addition of periodic torque, using periodic impulse input as a control torque, the delayed feedback control, external force

feedback control, Bang-Bang control, optimal control and adaptive control are used to control chaos.

Finally, attention is shifted to the synchronization and anticontrol of chaos. For synchronization of chaos, the chaotic system is decomposed into two subsystems proposed by Pecora and Carroll[5]. In the thesis, linear feedback, nonlinear feedback, adaptive feedback, backstepping design and parameter evaluation from time sequences approaches are discussed for synchronization of two coupled chaotic system, respectively. For anticontrol of chaos, two different procedure, linear and nonlinear controllers with certain feedback gain are proposed to anticontrol, i.e. to chaotify, the governor system.

Chapter 3

Chaotic Dynamics of the System

3.1 Chaos, Controlling Chaos and Synchronization of Chaos of Autonomous System

In nonlinear dynamical systems, variation of system parameters may cause sudden change in the qualitative behavior of their state. The state change is referred to as a bifurcation and the parameter value at which the bifurcation occurs is called the bifurcation value. Denoting $\phi = x, \dot{\phi} = y, \omega = z,$ equation (2.1.4) is rewritten in the form

$$\dot{x} = y$$
$$\dot{y} = dz^2 \cos x + \frac{1}{2}(e + pz^2)\sin 2x - \sin x - by$$
$$\dot{z} = q\cos x - F \tag{3.1.1}$$

The condition for the eigenvalues of Jacobian consisting of a pure imaginary pair and eigenvalue with negative real part can be shown to be

$$q_c = 2.2558$$

Here q is considered as the control parameter to be varied for the occurrence of Hopf bifurcation. q_c is the critical value when the values of parameters d, e, p, F, b are given as 0.08, 0.8, 0.04, 1.942, 0.4, respectively.

3.1.1 Phase Portraits , Poincaré Map and Power Spectrum

The phase portrait is the evolution of a set of trajectories emanating from various initial conditions in the state space. When the solution reaches steady state, the transient behavior disappears. The idea of transforming the

study of continuous systems into the study of an associated discrete system was presented by Henri Poincaré. One of many advantages of Poincaré map is to reduce dimensions of the dynamical system. The solution of period-1T in the phase plane will become one point in the Poincaré map. Usually, the period of the trajectories is not explicitly known for the autonomous system, so the choice of the Poincaré section is differ from the nonautonomous system. The Poincaré section of the three-dimensional autonomous system Eq. (3.1.1) is defined by

$$\Sigma = \left\{ (x, y, z) \in R \times R \times R \mid z = z_0 \right\}$$

and satisfies the condition

$$n \cdot (x - x_\Sigma) > 0$$

The vector n normal to Σ is given by

$$n = \begin{bmatrix} 0 \\ 0 \\ 1 \end{bmatrix}$$

and x_Σ is point located on the section Σ. As q is increased passing through the critical value 2.2558, the supercritical hopf bifurcation occurs, i.e., a stable fixed point becomes unstable and a stable limit cycle appears. Then a cascade of period-doubling bifurcations develops which leads the system into chaos. By using fourth order Runge-Kutta numerical integration method, the phase plane and Poincaré map of the system, equation (3.1.1), is plotted in Fig. 3.1(a), (b) for $q = 2.3$, 3, respectively. Clearly, the motion is periodic. But Fig. 3.1(c), (d) for $q = 5.5$ show the chaotic states. Because the Poincaré map is neither a finite set of points nor a closed orbit, the motion may be chaotic.

A valuable technique for the identification and characterization of the system is the power spectrum. This representation is useful for dynamical

analysis. The periodic motion of autonomous system are observed by the portraits of power spectrum in Fig. 3.2(a) for $q = 2.3$. The solution of system is period-1T, and the power spectrum exhibits a strong peak at the principal frequency

Apparently, the spectrum of the periodic motion only consists of discrete frequencies. As $q = 5.5$ chaos occurs, the spectrum is a continuous broad-band one shown in Fig. 3.2(b). The noise-like spectrum is the characteristic of chaotic dynamical system. Although a broad spectrum does not guarantee sensitivity to initial conditions, it is still a reliable indicator of the chaos.

3.1.2 Lyapunov Exponent and Lyapunov Dimension

The Lyapunov exponent may be used to measure the sensitive dependence upon initial conditions. It is an index for chaotic behavior. Different solutions of dynamical system, such as fixed points, periodic motions, quasiperiodic motion, and chaotic motion can be distinguished by it. In three dimensional space, the Lyapunov exponents for a strange attractor, a limit cycle and a fixed point are described by $(+,0,-)$, $(0,-,-)$ and $(-,-,-)$, respectively[15].

As $q = 2$, three Lyapunov exponents are obtained, respectively; $\lambda_1 = -0.0526, \lambda_2 = -0.0535, \lambda_3 = -0.2939$, which the motion converges to fixed point. For $q = 2.3$ and $q = 5.5$, the Lyapunov exponents are $\lambda_1 = 0, \lambda_2 = -0.1951, \lambda_3 = -0.205$ and $\lambda_1 = 0.0839, \lambda_2 = 0, \lambda_3 = -0.484$, respectively. The Lyapunov exponents of the solutions of the non-linear dynamical system, equation (3.1.1), are plotted in Fig. 3.3 as q ranges from 2 to 5.5. For the

dissipative system studied the sum of the three Lyapunov exponents is equivalent to the negative damping coefficient -0.4. If the value of the largest Lyapunov exponent is greater than zero, it is chaos, otherwise periodic solution.

There are a number of different fractional-dimension-like quantities, including the information dimension, Lyapunov dimension, and the correlation exponent, etc; the difference between them is often small. The Lyapunov dimension is a measure of the complexity of the attractor. It has been developed by Kaplan and Yorke [16] that the Lyapunov dimension d_L is introduced as

$$d_L = j + \frac{\sum_{i=1}^{j} \lambda_i}{\left| \lambda_{j+1} \right|},$$

where j is defined by the condition that

$$\sum_{i=1}^{j} \lambda_i > 0 \quad \text{and} \quad \sum_{i=1}^{j+1} \lambda_i < 0.$$

Therefore the Lyapunov dimension for a strange attractor is a non-integer number. By applying the technique, the Lyapunov dimension $d_L = 2.173$ with $q = 5.5$.

3.1.3 Controlling Chaos

Several interesting non-linear dynamic behaviors of the system have been discussed in previous sections. It has been shown that the autonomous system exhibited both regular and chaotic motion. Usually chaos is unwanted or undesirable. In order to improve the performance of a dynamic system or to avoid the chaotic phenomena, we need to control a chaotic motion to become a periodic motion which is beneficial for working with a particular condition. It is thus of great practical importance to develop suitable control methods. Much interest has been focused on this type of problem - controlling chaos [4,6,12].

For this purpose, open-loop strategies and close-loop feedback methods are used to control our system from chaos to order.

(1) Controlling Chaos by Delayed Feedback Control

Let us consider a dynamic system which can be simulated by ordinary differential equations. We imagine that the equations are unknown, but some scalar variable can be measured as a system output. The idea of this method, is that the difference *D(t)* between the delayed output signal $y(t - \tau)$ and the output signal *y(t)* is used as a control signal. In other word, we adapt a perturbation of the form [17]:

$$u(t) = K[y(t - \tau) - y(t)] = KD(t) \tag{3.1.2}$$

here τ is a delay time.

The difference between the delayed output signal and the output signal itself is used as a control signal. To achieve the periodic motion of the system, two parameters, namely, the time of delay τ and the weight *K* of the feedback, should be adjusted. For the autonomous system, it is easy to choose an appropriate τ to achieve the periodic state. From the simulation process, this method is more effective and applicable for control of chaos to the rotational machine. The numerical results are shown in Fig. 3.4 with *K* = 0.4.

(2) Controlling Chaos by Adaptive Control Algorithm (ACA)

A simple and effective adaptive control algorithm is suggested [18], which utilizes an error signal proportional to the difference between the goal output and actual output of the system. The error signal governs the change of parameters of the system, which readjusts so as to reduce the error to zero. This method can be explained briefly. The system motion is set back to a desired state X_s by adding dynamics on the control parameter *P* through the

evolution equation,

$$\dot{P} = \varepsilon G(X - X_s) \qquad (3.1.3)$$

where the function G depends on the difference between X_s and the actual output X, and ε indicates the stiffness of the control. The function G could be either linear or non-linear. In order to convert the dynamics of system (3.1.1) from chaotic motion to the desired periodic motion X_s, the chosen paramer q is perturbed as

$$\dot{q} = \varepsilon(X - X_S) \qquad (3.1.4)$$

if $\varepsilon = 0.005$, the system can reach the period-1 and period-2 easily shown as Fig. 3.5. It is clear that the desired periodic motion can be reached by adaptive control algorithm.

(3) Controlling Chaos by Linear Feedback Control

A linear feedback control with a special form is used in this method. It is assumed that the input signal *u(t)* disturbs only the third equation in (3.1.1). and

$$u(t) = K_2[y_i(t) - y(t)] = K_2 D(t)$$

Here, *y(t)* is the chaotic output signal, $y_i(t)$ is the periodic motion of system. The difference $D(t)$ between the signal $y_i(t)$ and $y(t)$ is used as a control signal. Here K_2 is an adjustable weight of the feedback. By selecting the weight K_2, we can convert chaotic behavior to periodic motion. We can control the chaotic behavior to period-1 motion by choosing $K_2 = 0.5$ as shown in Fig. 3.6.

(4) Controlling Chaos by Optimal Control

Optimal control is a well-established engineering control strategy, and is useful for both linear and nonlinear system with linear or nonlinear controllers [6]. Now, we use a typical optimal control for a chaos control. We consider the equation(3.1.1) with a controller u and define the Hamilton function :

$$H(x, y, z, u, p) = \boldsymbol{p}^T \boldsymbol{F}(x, y, z, u, t) \quad , \quad \boldsymbol{p}^T = [p_1 \ p_2 \ p_3]$$

Following the variation principle of optimal control, we can obtain

$$p_1 y + p_2 [dz^2 \cos x + \frac{1}{2}(e + pz^2)\sin 2x - \sin x - by] = 0 \qquad (3.1.5)$$

$$- p_2 (2dz \cos x + pz \sin 2x) = 0 \qquad (3.1.6)$$

This yield a non-trivial solution for (p_1, p_2) if and only if

$$2dz \cos x + pz \sin 2x = 0 \qquad (3.1.7)$$

It gives an optimal surface singularly in the state space. This type of control assumes values on the two allowable boundaries (3.1.5) and (3.1.6) alternatively according to a switching surface. Locating system trajectories on the surface, a typical feedback control in the form

$$u = -k_b \operatorname{sgn}[2dz \cos x + pz \sin 2x]$$

can be used. By adjusting the value of k_b in the above controller with the signum function

$$\operatorname{sgn}[v] = \begin{cases} 1 & \text{if} \quad v > 0 \\ 0 & \text{if} \quad v = 0 \\ -1 & \text{if} \quad v < 0 \end{cases}$$

the chaotic motion can be controlled to periodic motion which we desired by modulating the value of k_b. The simulation result is shown in Fig. 3.7 with $k_b = 1.5$.

3.1.4 Chaos Synchronization and Phase Synchronization

A characteristic property of chaotic dynamics is the sensitive dependence on initial condition. Different initial conditions will cause different trajectories for the system. However, a few years ago Pecora and Carroll [5] shown that synchronization can be achieved for the chaotic systems. This interest phenomenon plays a significant role in the chaotic dynamics of communication signals and may be applied to the real-time recovery of signals that have been masked in a strange attractor and thus to encode communication. Other applications of synchronization of chaos also have expectative potential [7,8]. A natural way to develop synchronization for chaotic systems is through system decomposition. The coupled systems are decomposed into two subsystem as follows :

$$\begin{cases} \dot{x}_1 = y_1 \\ \dot{y}_1 = dz_1^2 \cos x_1 + \frac{1}{2}(e + pz_1^2)\sin 2x_1 - \sin x_1 - by_1 \\ \dot{z}_1 = q\cos x_1 - F \end{cases} \quad \text{(drive)} \quad (3.1.8)$$

$$\begin{cases} \dot{x}_2 = y_2 \\ \dot{y}_2 = dz_2^2 \cos x_2 + \frac{1}{2}(e + pz_2^2)\sin 2x_2 - \sin x_2 - by_2 \\ \dot{z}_2 = q\cos x_2 - F \end{cases} \quad \text{(response)}(3.1.9)$$

In the following, several feedback based approaches are discussed.

(1) Linear Feedback Synchronization

In this approach, the error between the output of the identical drive and response is used as the control signal. The first equation of response(3.1.9) is combined with a linear feedback, while the equations of drive remain the same[6].

$$\begin{cases} \dot{x}_2 = y_2 + k(x_1 - x_2) \\ \dot{y}_2 = dz_2^2 \cos x_2 + \frac{1}{2}(e + pz_2^2)\sin 2x_2 - \sin x_2 - by_2 \\ \dot{z}_2 = q\cos x_2 - F \end{cases} \quad (3.1.10)$$

where k is the constant feedback gain. With k= 0.5, the trajectories of subsystems and the synchronization errors, $e_x = x_2 - x_1$, $e_y = y_2 - y_1$, and $e_z = z_2 - z_1$, are shown in Fig. 3.8. In this case, k= 0.38 is a critical value, below which no synchronization occurs.

(2)   Adaptive Feedback Synchronization

In section 3.1.3, adaptive control strategies can direct a chaotic trajectory to stable orbits but not unstable ones. Therefore, it is possible to combine the feedback method for chaos synchronization [6].

For response (3.1.9), the linear feedback (3.1.10) is replaced by

$$\dot{x}_2 = y_2 + k_1(x_1 - x_2)$$
$$\dot{q} = k_2(y_1 - y_2)$$

(3.1.11)

where q is the system parameter, and k_2 is a constant adaptive control gain to be determined in the design. Using this method, the response can synchronize the chaotic drive, as shown in Fig. 3.9.

(3)   Phase Synchronization

Recently, the concept of phase, as well as phase synchronization, has been discussed in detail for chaotic oscillators [19,20]. If we project the attractor on plane (x,y), it has one rotation center shown in Fig. 3.1(c) and Fig. 3.10. The phase of the system can be defined as :

$$\phi = \arctan \frac{y}{x}$$

(3.1.12)

The phase can be easily calculated for each subsystem. Phase synchronization occurs when the phases of two oscillators have the relationship $\phi_1(t) \approx \phi_2(t)$ with time. To determine the level of mismatch of phase synchronization, we use cross-correlation function $\xi(\tau)$ with time shift τ [20].

$$\xi(\tau) = \frac{\langle y_1(t) y_2(t + \tau)\rangle}{\left(\langle y_1^2(t)\rangle \langle y_2^2(t)\rangle\right)^{1/2}}$$

(3.1.13)

We study two coupled centrifugal governor systems with strength of coupling ε,

$$\dot{x}_{1,2} = y_{1,2}$$

$$\dot{y}_{1,2} = dz_{1,2}^2 \cos x_{1,2} + \frac{1}{2}(e + pz_{1,2}^2)\sin 2x_{1,2} - \sin x_{1,2} - by_{1,2} + \varepsilon(y_{2,1} - y_{1,2})$$

$$\dot{z}_{1,2} = q\cos x_{1,2} - F$$

(3.1.14)`

To examine phase synchronization, we modulate the coupling parameter ε in Eq. (3.1.14). Some numerical results are given in Fig. 3.11 with $0 < \varepsilon < 0.5$. Fig. 3.11(a) shows the maximum absolute difference of two phases. Obviously, the phases of two coupled systems are synchronizing in the region $\varepsilon > 0.193$. Fig. 3.11(b) shows the maximum absolute difference of two trajectories. When $\varepsilon > 0.193$, they are synchronization. Therefore, phase synchronization and full synchronization coincide for two coupled centrifugal governor systems. It means that the phases and amplitudes of two systems are equally correlated [20]. The cross-correlation function $\xi(0)$ with $\tau = 0$ is also shown in Fig. 3.11(c) correspondingly. It has been shown that phase synchronization for coupled Rössler systems is related to one of the zero Lyapunov exponents becoming negative [19]. But our simulation shows that there is not such a relationship for our system in Fig. 3.12. All signs of six Lyapunov exponents remain unchanged. This phenomenon indicates that a Lyapunov exponent decreasing from zero to negative cannot be used as a criterion for phase synchronization [20]. However, we can observe that when phase synchronization begins at $\varepsilon = 0.193$, one of negative Lyapunov exponents approaches to zero, and becomes immediately negative again when $\varepsilon > 0.193$ in Fig. 3.12.

21

3.2 Anticontrol and Synchronization of Chaos of Autonomous System

Anticontrol of chaos is making a nonchaotic dynamical system chaotic. This implies that the regular behaviors will be destroyed and replaced by chaotic behavior. In the real world, chaotic behavior is important. Examples include liquid mixing, humam heartbeat regulations, resonance prevention in mechanical systems and secure communication[11]. In this section, equation(3.1.1) are modified by the addition of a linear feedback and a nonlinear feedback to chaotify the system, respectively.

3.2.1 Adding a Linear Feedback

The state equations of the centrifugal governor system with a linear feedback controller are represented as

$$\dot{x} = y + a_1 x$$

$$\dot{y} = dz^2 \cos x + \frac{1}{2}(e + pz^2)\sin 2x - \sin x - by + a_2 y \qquad (3.2.1)$$

$$\dot{z} = q \cos x - F + a_3 z$$

Here a_1, a_2, a_3 are feedback gains and the values of parameters d, e, p, q, F, b are given as 0.008, 0.8, 0.04, 3, 2, 0.4, respectively.

By numerical integration method, the phase portrait of the system, equation (3.2.1), is plotted in Fig. 3.13 for $a_1 = a_2 = a_3 = 0$. Clearly, the motion is periodic. But equation (3.2.1) exhibits both strange attractors and limit cycles for certain choices of a_1, a_2 and a_3. For example, when $a_1 = 0.2, a_2 = -0.1, a_3 = -0.1$, one can observe a chaotic attractor as depicted in Fig. 3.14. By simulation results, for certain interval of parameters, the system

exhibits the strange attractor. Inspired by the consideration of chaotification, we found regions of specific feedback gains for which this system is chaotic as shown in Fig. 15.

3.2.2 Adding a Nonlinear Feedback

For our purpose, the nonlinear feedback controller, $\varepsilon x|x|$, is added to the right-hand side of the first equation of equation(3.1.1). Then the system equations are represented as

$$\dot{x} = y + \varepsilon x|x|$$

$$\dot{y} = dz^2 \cos x + \frac{1}{2}(e + pz^2)\sin 2x - \sin x - by \qquad (3.2.2)$$

$$\dot{z} = q \cos x - F$$

The system(3.2.2) is obtained which for certain value of ε (for example, $0.008 \le \varepsilon \le 0.032$) has strange attractor by numerical solution. As illustrated in Fig. 3.16, chaotic motion is observed from system(3.2.2) with $\varepsilon = 0.01$.

3.2.3 Chaos Synchronization

The chaotic system(3.2.1) is decomposed into two subsystems as follows :

drive system :

$$\dot{x}_1 = y_1 + 0.2x_1$$
$$\dot{y}_1 = dz_1^2 \cos x_1 + \frac{1}{2}(e + pz_1^2)\sin 2x_1 - \sin x_1 - by_1 - 0.1y_1 \qquad (3.2.3)$$
$$\dot{z}_1 = q \cos x_1 - F - 0.1z_1$$

response system:

$$\dot{x}_2 = y_2 + 0.2x_2$$
$$\dot{y}_2 = dz_2^2 \cos x_2 + \frac{1}{2}(e + pz_2^2)\sin 2x_2 - \sin x_2 - by_2 - 0.1y_2 \qquad (3.2.4)$$
$$\dot{z}_2 = q \cos x_2 - F - 0.1z_2$$

In the following, linear feedback, nonlinear feedback, adaptive feedback and backstepping design approaches are discussed.

(1) Linear Feedback Synchronization

In this approach, the error between the output of the identical drive and response is used as the control signal. For the unidirectional case, where only first equation of response system(3.2.4) is combined with a linear feedback, while the equations of drive remain the same[5].

$$\dot{x}_2 = y_2 + 0.2x_2 + k_1(x_1 - x_2)$$
$$\dot{y}_2 = dz_2{}^2 \cos x_2 + \frac{1}{2}(e + pz_2{}^2)\sin 2x_2 - \sin x_2 - by_2 - 0.1y_2 \qquad (3.2.5)$$
$$\dot{z}_2 = q \cos x_2 - F - 0.1z_2$$

where k_1 is the constant feedback gain. With $k_1 = 0.2$, the synchronization errors, $e_x = x_2 - x_1$, $e_y = y_2 - y_1$, and $e_z = z_2 - z_1$, are shown in Fig. 3.17. In this case, $k_1 = 0.15$ is a critical value, below which no completely synchronization occurs.

(2) Nonlinear Feedback Synchronization

The chaotic response system(3.2.4) by adding nonlinear coupling term are written as

$$\dot{x}_2 = y_2 + 0.2x_2 + k_2 \sin(x_1 - x_2)$$
$$\dot{y}_2 = dz_2{}^2 \cos x_2 + \frac{1}{2}(e + pz_2{}^2)\sin 2x_2 - \sin x_2 - by_2 - 0.1y_2 \qquad (3.2.6)$$
$$\dot{z}_2 = q \cos x_2 - F - 0.1z_2$$

With $k_2 = 0.2$, the synchronization errors are shown in Fig. 3.18. In this case, $k_2 = 0.15$ is a critical value, below which no completely synchronization occurs.

(3) Adaptive Feedback Synchronization

Some adaptive control strategies can direct a chaotic trajectory to stable orbits but not unstable ones. However, it is possible to combine the feedback method for chaos synchronization [21,22].

For response system(3.2.4), the linear feedback (3.2.5) is replaced by

$$\dot{x}_2 = y_2 + 0.2x_2 + k_3(x_1 - x_2)$$

$$\dot{y}_2 = dz_2{}^2 \cos x_2 + \frac{1}{2}(e + pz_2{}^2)\sin 2x_2 - \sin x_2 - by_2 - 0.1y_2$$

$$\dot{z}_2 = q\cos x_2 - F - 0.1z_2$$

$$\dot{q} = k_4(y_1 - y_2)$$

(3.2.7)

where the system parameter q is used as an adjustable function for adaptation, and k_4 is a constant adaptive control gain to be determined in the design. Using this method, the response can be synchronized by the chaotic drive, as shown in Fig. 3.19.

(4) Backstepping design

Backstepping design is a recursive procedure that combines the choice of a Lyapunov function for selecting a proper controller in chaos synchronization[23]. The drive system is expressed as Eq.(3.2.3) and a controller u is added to the right-hand side of the second equation of response system(3.2.4). Let the state errors between the response system and drive system be

$$e_x = x_2 - x_1 \qquad e_y = y_2 - y_1 \qquad e_z = z_2 - z_1$$

(3.2.8)

then error system can be derived as

$$\dot{e}_x = e_y + 0.2e_x$$

$$\dot{e}_y = d[\cos x_2(e_z^2 + 2z_1e_z) + \frac{z_1^2}{2}(e_x^2 + 2x_1e_x)] + (e-1)e_x$$

$$\qquad + \frac{p}{2}[\sin 2x_2(e_z^2 + 2z_1e_z) + 2z_1^2e_x] - (b+0.1)e_y + u + h.o.t.$$

(3.2.9)

$$\dot{e}_z = \frac{q}{2}e_x - 0.1e_z$$

If system(3.2.9) did not have u, it would have an equilibrium point(0,0,0). The problem of synchronization between drive and response system can be transformed into how to find a control law u for stabilizing the error variables

of system(3.2.9) at the origin.

First we consider the stability of system as following :

$$\dot{e}_z = \frac{q}{2} e_x - 0.1 e_z \tag{3.2.10}$$

where e_x is regarded as a controller and it makes system(3.2.10) asymptotically stable. Choose Lyapunov function $V_1(e_z) = e_z^2 / 2$. The derivative of V_1 is

$$\dot{V}_1 = -0.1 e_z^2 + \frac{q}{2} e_z e_x \tag{3.2.11}$$

Assume controller $e_x = \alpha_1(e_z)$ and $\alpha_1(e_z) = 0$, then

$$\dot{V}_1 = -0.1 e_z^2 < 0 \tag{3.2.12}$$

makes system(3.2.10) asymptotically stable. Function $\alpha_1(e_z)$ is an estimative function when e_x is considered as a controller. The error between e_x and $\alpha_1(e_z)$ is

$$w_2 = e_x - \alpha_1(e_z) \tag{3.2.13}$$

Study (e_z, w_2) system

$$\begin{aligned} \dot{e}_z &= \frac{q}{2} w_2 - 0.1 e_z \\ \dot{w}_2 &= e_y + 0.2 w_2 \end{aligned} \tag{3.2.14}$$

Consider $e_y = \alpha_2(e_z, w_2)$ as a controller in system(3.2.14). Choose Lyapunov function $V_2(e_z, w_2) = V_1(e_z) + w_2^2 / 2$. The derivative of V_2 is

$$\dot{V}_2 = -0.1 e_z^2 + 0.2 w_2^2 + \frac{q}{2} w_2 e_z + w_2 e_y \tag{3.2.15}$$

If $\alpha_2(e_z, w_2) = -\frac{q}{2} e_z - w_2$, then

$$\dot{V}_2 = -0.1 e_z^2 - 0.8 w_2^2 < 0 \tag{3.2.16}$$

makes system(3.2.14) asymptotically stable. Define the error variable w_3 as

$$w_3 = e_y - \alpha_2(e_z, w_2) \tag{3.2.17}$$

Study full dimension (e_z, w_2, w_3) system

$$\dot{e}_z = \frac{q}{2} w_2 - 0.1 e_z$$

$$\dot{w}_2 = w_3 + \alpha_2 + 0.2 w_2$$

$$\dot{w}_3 = d[\cos x_2 (e_z^2 + 2z_1 e_z) + \frac{z_1^2}{2}(w_2^2 + 2x_1 w_2)] + (e-1)w_2 - (b+0.1)(w_3 + \alpha_2)$$

$$+ \frac{p}{2}[\sin 2x_2 (e_z^2 + 2z_1 e_z) + 2z_1^2 w_2] - \frac{d\alpha_2}{dt} + u + h.o.t.$$

$$\tag{3.2.18}$$

where

$$\frac{d\alpha_2}{dt} = -\frac{q}{2}(\frac{q}{2} w_2 - 0.1 e_z) - (w_3 + \alpha_2 + 0.2 w_2)$$

Choose Lyapunov function $V_3(e_z, w_2, w_3) = V_2(e_z, w_2) + w_3^2 / 2$. The derivative of

V_3 is

$$\dot{V}_3 = -0.1 e_z^2 - 0.8 w_2^2 + w_3[2z_1 e_z (q\cos x_2 + \frac{p}{2}\sin 2x_2) + e w_2$$

$$\tag{3.2.19}$$

$$- (b+0.1)(w_3 + \alpha_2) + \frac{dz_1^2}{2}(w_2^2 + 2x_1 w_2) + pz_1^2 w_2 - \frac{d\alpha_2}{dt} + u] + h.o.t.$$

Let

$$u = (b+0.1)\alpha_2 - 2z_1 e_z (q\cos x_2 + \frac{p}{2}\sin 2x_2) - e w_2$$

$$- \frac{dz_1^2}{2}(w_2^2 + 2x_1 w_2) - pz_1^2 w_2 + \frac{d\alpha_2}{dt}$$

then

$$\dot{V}_3 = -0.1 e_z^2 - 0.8 w_2^2 - (b+0.1)w_3^2 + h.o.t.$$

is quadric negative definite. Whereas x_1, z_1 and x_2 are bounded, we can

conclude that the equilibrium point(0,0,0) of error system(3.2.9) is locally

asymptotically stable. For proper initial errors between drive and response

systems, the initial errors will converge to zero and synchronization between

two chaotic subsystems will be achieved. The numerical results with initial condition ($x_1(0) = 1.42$, $y_1(0) = -2.1$, $z_1(0) = 5.55$, $x_2(0) = 1.4$, $y_2(0) = -2$, $z_2(0) = 5.5$) are shown in Fig. 3.20.

(5) Parameter evaluation from time sequences

In this section, we study another method to estimate the parameter of chaotic system by a random optimization method for chaos synchronization[24]. For system(3.2.5), q is the unknown parameter and k_1 is a coupling constant. The difference of the two time sequences is calculated as

$$U = \int_0^T |x_2 - x_1|^2 dt$$

the integral time T is larger than a typical period of the chaotic oscillation in the governor system and the parameter q is randomly modified as

$$q' = q + \zeta$$

where ζ is a random number. We can obtain a time sequence $x'_2(t)$ by numerical simulation of Eq.(3.2.5) with the modified parameter q'. Then the difference of the two time sequences is calculated as

$$U' = \int_0^T |x'_2 - x_1|^2 dt$$

If the difference U' is smaller than U, the parameter is changed from q to q'. On the other hand, if the difference U' is larger than U, the parameter is unchanged and kept to be q. The obtained parameter value is expected to be the desired parameter until the difference U becomes zero, i.e., complete chaos synchronization is achieved.

Fig. 3.21 displays the minimum value of U with respect to the coupling constant k_1. The numerical simulation shows that the complete chaos synchronization $x_2(t) = x_1(t)$ occurs for $k_1 > 0.15$. This result is the same as that in section 3.2.3 (1). The difference U as a function of the parameter q for

$k_1 = 0.2$ is shown in Fig. 3.22. The complete chaos synchronization is attained when the value of U takes a minimum value 0 at $q = 3$. Time evolution of the parameter q by the random optimization process is shown in Fig. 3.23.

3.3 Chaos, Control, Anticontrol and Synchronization of Chaos for the System with Time-Delay

Chaos, control, anticontrol and synchronization of chaos for an autonomous rotational machine system with a hexagonal centrifugal governor and spring for which time-delay effect is considered are studied in this section. For a mass-spring system shown in Fig. 3.24, suppose m is not a particle. It has a length $P_2 - P_1$. When the spring force acts on m at P_1 in some instant t, m does not move immediately. This is because that when a force acts on the surface P_1 of m, the stress waves propagate inside m. Usually the stress waves start from P_1 and reflected at P_2. After crisscross of stress waves inside m, acceleration of m becomes uniform, and m begins to move actually at this time. Let the time interval between the instant of exertion of the force on m and the instant at which m moves actually be τ. We have the equation of motion of time delay system as $m\ddot{x}(t) + kx(t-\tau) = 0$. This kind of time delay is considered in this section.

3.3.1 Regular and Chaotic Dynamics of Time-Delay System

The governor system(2.1.4) with time-delay considered can be modeled by the following delay differential equations:

$$\dot{\phi} = \varphi$$

$$\dot{\varphi} = \frac{r}{l}\omega^2 \cos\phi + \omega^2 \sin\phi\cos\phi - \frac{2k}{m}(1 - \cos\phi_{t-\tau})\sin\phi - \frac{g}{l}\sin\phi - c\varphi \quad (3.3.1)$$

$$\dot{\omega} = q\cos\phi - F$$

29

In nonlinear dynamical systems, variation of system parameters may cause sudden change in the qualitative behavior of their state. The state change is referred to as a bifurcation and the parameter value at which the bifurcation occurs is called the bifurcation value. Denoting $\phi = x, \dot{\phi} = y, \omega = z,$ equation (3.3.1) is rewritten in the form

$$\dot{x} = y$$

$$\dot{y} = \frac{r}{l} z^2 \cos x + z^2 \sin x \cos x - \frac{2k}{m}(1 - \cos x_{t-\tau}) \sin x - \frac{g}{l} \sin x - cy \qquad (3.3.2)$$

$$\dot{z} = q \cos x - F$$

Here q is considered as the control parameter to be varied when the values of parameters r, l, k, m, F, c are given as 0.4, 2, 20, 2, 1.942, 0.4, respectively.

The phase portrait is the evolution of a set of trajectories emanating from various initial conditions in the state space. When the solution reaches steady state, the transient behavior disappears. By numerical integration method, the phase portrait of the system, equation (3.3.2), is plotted in Fig. 3.25(a) for $q = 3$. Clearly, the motion is periodic. But Fig. 3.25(b) for $q = 5.5$ shows the chaotic states. Furthermore the power spectrum is a continuous broad-band one shown in Fig. 3.26(b) as $q = 5.5$. The noise-like spectrum is the characteristic of chaotic dynamical system.

3.3.2 Controlling Chaos

It has been shown that the time-delay autonomous system exhibited both regular and chaotic motion in previous section. Usually chaos is unwanted or undesirable. In order to improve the performance of a dynamic system or to avoid the chaotic phenomena, we need to control a chaotic motion to become a periodic motion which is beneficial for working with a particular condition. For

this purpose, two methods are used to control the time-delay system from chaos to order.

(1) Controlling Chaos by Adaptive Control Algorithm (ACA)

A simple and effective adaptive control algorithm is suggested [18], which utilizes an error signal proportional to the difference between the goal output and actual output of the system. The error signal governs the change of parameters of the system, which readjusts so as to reduce the error to zero. This method can be explained briefly. The system motion is set back to a desired state X_s by adding dynamics on the control parameter P through the evolution equation,

$$\dot{P} = \varepsilon G(X - X_s) \tag{3.3.3}$$

where the function G depends on the difference between X_s and the actual output X, and ε indicates the stiffness of the control. The function G could be either linear or non-linear. In order to convert the dynamics of system (3.3.2) from chaotic motion to the desired periodic motion X_s, the chosen paramer q is perturbed as

$$\dot{q} = K_1(X - X_S) \tag{3.3.4}$$

If $K_1=0.5$, the system can reach the period-1 easily shown as Fig. 3.27. It is clear that the desired periodic motion can be reached by adaptive control algorithm.

(2) Controlling Chaos by Linear Feedback Control

A linear feedback control with a special form is used in this method. It is assumed that the input signal *u(t)* disturbs only the third equation in (3.3.2). and

$$u(t) = K_2[y_i(t) - y(t)] = K_2 D(t) \tag{3.3.5}$$

Here, $y(t)$ is the chaotic output signal, $y_i(t)$ is the periodic motion of system.

The difference $D(t)$ between the signal $y_i(t)$ and $y(t)$ is used as a control signal. Here K_2 is an adjustable weight of the feedback. By selecting the weight K_2, we can convert chaotic behavior to periodic motion. We can control the chaotic behavior to period-1 and period-2 motion by choosing $K_2=5$ and 0.5, respectively, as shown in Fig. 3.28.

3.3.3 Chaos Synchronization

The chaotic system is decomposed into two subsystems as follows :

drive system:

$$\dot{x}_1 = y_1$$

$$\dot{y}_1 = \frac{r}{l}z_1^2 \cos x_1 + z_1^2 \sin x_1 \cos x_1 - \frac{2k}{m}(1-\cos x_{1t-\tau})\sin x_1 - \frac{g}{l}\sin x_1 - cy_1 \quad (3.3.6)$$

$$\dot{z}_1 = q\cos x_1 - F$$

response system:

$$\dot{x}_2 = y_2$$

$$\dot{y}_2 = \frac{r}{l}z_2^2 \cos x_2 + z_2^2 \sin x_2 \cos x_2 - \frac{2k}{m}(1-\cos x_{2t-\tau})\sin x_2 - \frac{g}{l}\sin x_2 - cy_2$$

$$\dot{z}_2 = q\cos x_2 - F \quad (3.3.7)$$

In the following, linear and nonlinear feedback based approaches are discussed.

(1) Linear Feedback Synchronization

In this approach, the error between the output of the identical drive and response is used as the control signal. For the unidirectional case, where only first equation of response(3.3.7) is combined with a linear feedback, while the equations of drive remain the same.

$$\dot{x}_2 = y_2 + K(x_1 - x_2)$$

32

$$\dot{y}_2 = \frac{r}{l} z_2{}^2 \cos x_2 + z_2{}^2 \sin x_2 \cos x_2 - \frac{2k}{m}(1 - \cos x_{2t-\tau}) \sin x_2 - \frac{g}{l} \sin x_2 - cy_2$$

$$\dot{z}_2 = q \cos x_2 - F \tag{3.3.8}$$

where K is the constant feedback gain. With $K= 3$, the trajectories of subsystems and the synchronization errors, $e_x = x_2 - x_1$, $e_y = y_2 - y_1$, and $e_z = z_2 - z_1$, are shown in Fig. 3.29. In this case, $K= 2.75$ is a critical value, below which no synchronization occurs.

Then we consider the two identical systems which are coupled together. The mutually coupled chaotic systems by adding linear coupling term are written as

drive system:

$$\dot{x}_1 = y_1 + K(x_2 - x_1)$$

$$\dot{y}_1 = \frac{r}{l} z_1{}^2 \cos x_1 + z_1{}^2 \sin x_1 \cos x_1 - \frac{2k}{m}(1 - \cos x_{1t-\tau}) \sin x_1 - \frac{g}{l} \sin x_1 - cy_1 \tag{3.3.9}$$

$$\dot{z}_1 = q \cos x_1 - F$$

response system:

$$\dot{x}_2 = y_2 + K(x_1 - x_2)$$

$$\dot{y}_2 = \frac{r}{l} z_2{}^2 \cos x_2 + z_2{}^2 \sin x_2 \cos x_2 - \frac{2k}{m}(1 - \cos x_{2t-\tau}) \sin x_2 - \frac{g}{l} \sin x_2 - cy_2$$

$$\dot{z}_2 = q \cos x_2 - F \tag{3.3.10}$$

The simulation result show that generalized synchronization occurs when $K = 0.8 \sim 2.75$, and two chaotic systems are complete synchronization when $K > 3.75$. With $K= 1.5$ and 3, the synchronization errors are shown in Fig. 3.30 and Fig. 3.31, respectively.

(2) Nonlinear Feedback Synchronization

The mutually coupled chaotic systems by adding nonlinear coupling term are written as

drive system:

$$\dot{x}_1 = y_1 + K\sin(x_2 - x_1)$$

$$\dot{y}_1 = \frac{r}{l}z_1{}^2\cos x_1 + z_1{}^2\sin x_1\cos x_1 - \frac{2k}{m}(1-\cos x_{1t-\tau})\sin x_1 - \frac{g}{l}\sin x_1 - cy_1$$

(3.3.11)

$$\dot{z}_1 = q\cos x_1 - F$$

response system:

$$\dot{x}_2 = y_2 + K\sin(x_1 - x_2)$$

$$\dot{y}_2 = \frac{r}{l}z_2{}^2\cos x_2 + z_2{}^2\sin x_2\cos x_2 - \frac{2k}{m}(1-\cos x_{2t-\tau})\sin x_2 - \frac{g}{l}\sin x_2 - cy_2$$

$$\dot{z}_2 = q\cos x_2 - F$$

(3.3.12)

With $K= 1.5$, the trajectories of subsystems and the synchronization errors are shown in Fig. 3.32.

(3) Phase Synchronization

Recently, the concept of phase, as well as phase synchronization, has been discussed in detail for chaotic oscillators [19,20]. If we project the attractor on plane (x,y), it has one rotation center shown in Fig. 3.25(b). The phase of the system can be defined as :

$$\phi = \arctan\frac{y - y_c}{x - x_c}$$

(3.3.13)

where the point (x_c, y_c) is the rotation center. The phase can be easily calculated for each subsystem, and the mean frequency also defined as [10]

$$\Omega = <\dot{\phi}> = \lim_{T\to\infty}\frac{\phi(T) - \phi(0)}{T}$$

(3.3.14)

Phase synchronization occurs when the phases of two oscillators have the relationship $\phi_1(t) \approx \phi_2(t)$ with time, i.e., frequency-locking state for $\Delta\Omega = \Omega_1 - \Omega_2 \to 0$.

We study two coupled centrifugal governor systems with strength of

coupling K,

$$\dot{x}_{1,2} = y_{1,2} + K(x_{2,1} - x_{1,2})$$

$$\dot{y}_{1,2} = \frac{r}{l} z_{1,2}^2 \cos x_{1,2} + z_{1,2}^2 \sin x_{1,2} \cos x_{1,2} - \frac{2k}{m}(1 - \cos x_{1,2_{t-\tau}}) \sin x_{1,2}$$
$$\qquad - \frac{g}{l} \sin x_{1,2} - c y_{1,2}$$
$$\tag{3.3.15}$$

$$\dot{z}_{1,2} = q \cos x_{1,2} - F$$

To examine phase synchronization, we modulate the coupling parameter K in Eq. (3.3.15). Some numerical results are given in Fig. 3.33. For the unidirectional case, Fig. 3.33(a) shows the maximum absolute difference of mean frequency between two trajectories. Obviously, the phases of two systems are synchronizing in the region $K > 3.9$. Fig. 3.33(b) shows the maximum absolute difference of mean frequency between the mutually coupled chaotic systems. When $K > 1.4$, they are phase synchronization. Therefore, phase synchronization is easily achieved in mutually coupled chaotic systems.

3.3.4 Anticontrol of Chaos

Sometimes, chaos is not only useful but actually important. Besides secure communication and information processing, chaos is desirable in many applications of liquid mixing while the required energy is minimized. For this purpose, making a non-chaotic dynamical system chaotic is called "anticontrol of chaos". For our system(3.3.2), it is periodic motion with q = 3. The feedback controller used is a simple triangle function shown in Fig. 3.34(a), the period motion becomes chaotic shown in Fig. 3.34(b).

3.4 Chaos, Controlling Chaos and Synchronization of Chaos of Nonautonomous System

3.4.1 Regular and Chaotic Dynamics of Nonautonomous System

In previous sections, the load torque is assumed to be constant for the system. Another condition can be considered. The load torque is now not constant but is represented by a constant term and a harmonic term $F + a\sin\overline{\omega}t$, where $F, a, \overline{\omega}$ are constants. Equation (3.1.1) is rewritten in the form

$$\dot{x} = y$$
$$\dot{y} = dz^2\cos x + \frac{1}{2}(e + pz^2)\sin 2x - \sin x - by$$
$$\dot{z} = q\cos x - F - a\sin\overline{\omega}t \qquad (3.4.1)$$

where $d = 0.008, e = 0.8, p = 0.04, F = 1.942, a = 0.6, b = 0.4, \overline{\omega} = 1.0$.

(1)Phase Portraits , Poincaré Map and Power Spectrum

The phase portrait is the evolution of a set of trajectories emanating from various initial conditions in the state space. When the solution reaches steady state, the transient behavior disappears. The idea of transforming the study of continuous systems into the study of an associated discrete system was presented by Henri Poincaré. One of many advantages of Poincaré map is to reduce dimensions of the dynamical system. The solution of period-1T in the phase plane will become one point in the Poincaré map. By using fourth order Runge-Kutta numerical integration method, the phase plane and Poincaré map of the system, equation (3.4.1), is plotted in Fig. 3.35(a), (b) for $q = 2.07, 2.14$, respectively. Clearly, the motion is periodic. But Fig. 3.35(c), (d) for $q = 2.21$ show the chaotic states. Because the Poincaré map is neither a finite set of points nor a closed orbit, the motion may be chaotic.

A valuable technique for the identification and characterization of the system is the power spectrum. This representation is useful for dynamical

analysis. The periodic motion of nonautonomous system are observed by the portraits of power spectrum in Fig. 3.36(a) for $q = 2.07$. The solution of system is period-1T, and the power spectrum exhibits a strong peak at the forcing frequency together with super-harmonic frequencies. As the q increase, the period-1T changes to period-2T and the peak arises at one half forcing frequency, twice of principal period in the power spectrum.

Apparently, the spectrum of the periodic motion only consists of discrete frequencies. As $q = 2.21$ chaos occurs, the points of Poincaré map become obviously irregular. The spectrum is a broad band and the peak is still presented at the fundamental frequency shown in Fig. 3.36(b). The noise-like spectrum is the characteristic of chaotic dynamical system.

(2) Bifurcation Diagram and Parametric Diagram

In the previous section, the information about the dynamics of the non-linear system for specific values of the parameters is provided. The dynamics may be viewed more completely over a range of parameter value. As the parameter is changed, the equilibrium points can be created or destroyed, or their stability can be lost. The phenomenon of sudden change in the motion as a parameter is varied is called bifurcation, and the parameter values at which they occur are called bifurcation points.

The bifurcation diagram of the non-linear system of equation (3.4.1) is depicted in Fig. 3.37. It is calculated by the fourth order Runge-Kutta numerical integration and plotted against the $q \in [2.07, 2.21]$ with the incremental value of q is 0.0002. At each q, the points of Poincaré map in the transient state of motion are discarded. The period-doubling bifurcation first appears for $q \approx 2.095$. In this model, a sequence of period-doubling bifurcations occurs and leads to chaos as the system parameter is varied.

Further, the parameter values, damping coefficient and forcing frequency will also be varied to observe the behaviors of bifurcation of the system. By varying simultaneously any two of the three parameters, amplitude of the external torque, damping coefficient, and forcing frequency, the parametric diagrams are described and shown as Fig. 3.38(a), (b). The enriched information of the behaviors of the system can be obtained from the diagrams.

(3) Lyapunov Exponent and Lyapunov Dimension

The Lyapunov exponent may be used to measure the sensitive dependence upon initial conditions. It is an index for chaotic behavior. Different solutions of dynamical system, such as fixed points, periodic motions, quasiperiodic motion, and chaotic motion can be distinguished by it. If two chaotic trajectories start close to one another in phase space, they will move exponentially away from each other for small times on the average. Thus, if d_0 is a measure of the initial distance between the two starting points, the distance is $d(t) = d_0 2^{\lambda t}$. The symbol λ is called Lyapunov exponent. The divergence of chaotic orbits can only be locally exponential, because if the system is bounded, $d(t)$ cannot grow to infinity. A measure of this divergence of orbits is that the exponential growth at many points along a trajectory has to be averaged. When $d(t)$ is too large, a new 'nearby' trajectory $d_0(t)$ is defined. The Lyapunov exponent can be expressed as:

$$\lambda = \frac{1}{t_N - t_0} \sum_{k=1}^{N} \log_2 \frac{d(t_k)}{d_0(t_{k-1})}.$$

The signs of the Lyapunov exponents provide a qualitative picture of a system dynamics. The criterion is

$\lambda > 0$ (chaotic),

$\lambda \leq 0$ (regular motion).

The periodic and chaotic motions can be distinguished by the bifurcation diagram, while the quasiperiodic motion and chaotic motion may be confused. However, they can be distinguished by the Lyapunov exponent method. The Lyapunov exponents of the solutions of the non-linear dynamical system, equation (3.4.1), are plotted in Figure 3.39 as q ranges from 2.07 to 2.21. For the system studied the sum of the four Lyapunov exponents is equivalent to the negative damping coefficient -0.4. If the value of Lyapunov exponent is greater than zero, it is chaos, otherwise periodic solution. Observably, the chaotic motion can be found in Fig. 3.39 for q close to 2.2.

There are a number of different fractional-dimension-like quantities, including the information dimension, Lyapunov dimension, and the correlation exponent, etc; the difference between them is often small. The Lyapunov dimension is a measure of the complexity of the attractor. It has been developed by Kaplan and Yorke that the Lyapunov dimension d_L is introduced as

$$d_L = j + \frac{\sum_{i=1}^{j} \lambda_i}{\left| \lambda_{j+1} \right|},$$

where j is defined by the condition that

$$\sum_{i=1}^{j} \lambda_i > 0 \quad \text{and} \quad \sum_{i=1}^{j+1} \lambda_i < 0.$$

The Lyapunov dimension for a strange attractor is a non-integer number. The Lyapunov dimension and the Lyapunov exponent of the non-linear system are listed in Table 1 for different value of q.

Table 1 Lyapunov exponents and Lyapunov dimensions of the system for different q

q	λ_1	λ_2	λ_3	λ_4	$\sum \lambda_i$	d_L	
2.07	-0.0431	0	-0.0437	-0.3132	-0.4	1	Period-1
2.14	-0.0407	0	-0.0553	-0.304	-0.4	1	Period-2
2.185	-0.0506	0	-0.0764	-0.273	-0.4	1	Period-4
2.21	0.0351	0	-0.1206	-0.3145	-0.4	2.291	Chaos

3.4.2 Controlling Chaos

Several interesting non-linear dynamic behaviors of the system have been discussed in previous sections. It has been shown that the forced system exhibited both regular and chaotic motion. Usually chaos is unwanted or undesirable.

In order to improve the performance of a dynamic system or to avoid the chaotic phenomena, we need to control a chaotic motion to become a periodic motion which is beneficial for working with a particular condition. It is thus of great practical importance to develop suitable control methods. Very recently much interest has been focused on this type of problem - controlling chaos. For this purpose, open-loop strategies and close-loop feedback methods are used to control our system from chaos to order.

(1) Controlling Chaos by Addition of Constant Motor Torque

Interestingly, one can even add just a constant term to control or quench the chaotic attractor to a desired periodic one in typical non-linear nonautonomous system. In practice, An external input u is a torque on the axis of rotational machine. The equation (3.4.1) can be rewritten as

$$\dot{x} = y$$
$$\dot{y} = dz^2 \cos x + \frac{1}{2}(e + pz^2)\sin 2x - \sin x - by$$
$$\dot{z} = q \cos x - F - a \sin \overline{\omega} t + u \tag{3.4.2}$$

It ensures effective control in a very simple way. In order to understand this simple controlling approach in a better way, this method is applied to the system (3.4.2) numerically. We add the constant motor torque u=T into the third equation of equation (3.4.2).

In the absence of the constant motor torque, the system exhibits chaotic behavior under the parameter condition, $q = 2.21$.

If one considers the effect of the constant motor torque T by increasing it from zero upwards, the chaotic behavior is then altered. In Fig. 3.40, the bifurcation diagram is shown. It is clear that the system returns to regular motion, when the constant motor torque T is great than 0.03.

(2) Controlling Chaos by the Addition of Periodic Force

One can control system dynamics by addition of external periodic force in the chaotic state. For our purpose, the added periodic force, $u = v\sin\tilde{\omega}t$, is given, the system can then be investigated by numerical solution, with the remaining parameter fixed. We examine the change in the dynamics of the system as a function of v for fixed $\tilde{\omega} = 2$. The bifurcation diagram is shown in Fig. 3.41. It presents the return of the chaotic behavior to periodic motion while the value of v increase form zero upward.

(3) Controlling Chaos by the Addition of Periodic Impulse Input

Following the sense of previous sections, another open loop control method is given. A technique for suppressing chaos is to apply a periodic impulse input to the system[6]. Consider the system of the form (3.4.2) and assume that the system is controlled by a periodic impulse input

$$u = \rho \sum_{i=0}^{\infty} \delta(\tau - iT_d) \tag{3.4.3}$$

where ρ is a constant impulse intensity, T_d is the period between two

consecutive impulses, and δ is the standard delta function. With different values of ρ and T_d the controlled system can be stabilized at different periodic orbits. For example, we fix the parameter $T_d = 0.01$ and adjust impulse intensity ρ, the chaotic behavior disappear. The bifurcation diagram is shown in Fig. 3.42.

(4) Controlling Chaos by Delayed Feedback Control

Let us consider a dynamic system which can be simulated by ordinary differential equations. We imagine that the equations are unknown, but some scalar variable can be measured as a system output. The idea of this method, is that the difference *D(t)* between the delayed output signal $y(t-\tau)$ and the output signal *y(t)* is used as a control signal. In other word, we adapt a perturbation of the form[17]:

$$u(t) = K[y(t-\tau) - y(t)] = KD(t) \qquad (3.4.4)$$

Here τ is a delay time. Choose an appropriate weight *K* and τ of the feedback one can achieve the periodic state. We can control the chaotic motion to any assigned periodic motion rapidly by this method. The dependence of the bifurcation diagram on *K* for period-1 time delay is shown in Fig. 3.43.

This control is achieved by the use of the output signal, which is fed in a special form into the system. The difference between the delayed output signal and the output signal itself is used as a control signal. Only a simple delay line is required for this feedback control. To achieve the periodic motion of the system, two parameters, namely, the time of delay τ and the weight *K* of the feedback, should be adjusted. From the simulation process, this method is more effective and applicable for control of chaos to the rotational machine.

(5) Controlling Chaos by Adaptive Control Algorithm (ACA)

Recently a simple and effective adaptive control algorithm is suggested, which utilizes an error signal proportional to the difference between the goal output and actual output of the system. The error signal governs the change of parameters of the system, which readjusts so as to reduce the error to zero. This method can be explained briefly. The system motion is set back to a desired state X_s by adding dynamics on the control parameter P through the evolution equation,

$$\dot{P} = \varepsilon G(X - X_s) \tag{3.4.5}$$

where the function G depends on the difference between X_s and the actual output X, and ε indicates the stiffness of the control. The function G could be either linear or non-linear. In order to convert the dynamics of system (3.4.1) from chaotic motion to the desired periodic motion X_s, the chosen paramer q is perturbed as

$$\dot{q} = \varepsilon(X - X_S) \tag{3.4.6}$$

if $\varepsilon = 0.2$, the system can reach the period-1 and period-2 easily shown as Fig. 3.44 and Fig. 3.45. It is clear that the desired periodic motion can be reached by adaptive control algorithm.

(6) Controlling Chaos by Bang-Bang Control

Define error function as follow:

$$e(t) = X(t) - X(t - T) \tag{3.4.7}$$

where T is the external torque frequency. Define $V(t) = e(t)^2$ which is always positive or zero.

$$\dot{V} = 2 \cdot e(t) \cdot \dot{e}(t)$$

If $\dot{V} < 0$ then V will approach zero, i.e. $e(t) \to 0$. It means that $x(t)$ approaches $x(t - T_i)$ and the periodic behavior is achieved. The control law can be determined as follow:

$$\dot{x} = F_1(x, y, z, t)$$

$$\dot{y} = F_2(x, y, z, t)$$

$$\dot{z} = F_3(x, y, z, t) + u \qquad (3.4.8)$$

if $\|e(t)\| \leq \delta$, $u(t) = 0$

else if $\|e(t)\| > \delta$ then

$$u(t) = -K_1 |F_3(x, y, z, t) - \dot{z}(t - T)| \qquad \text{when} \quad e(t) > 0$$

$$u(t) = K_1 |F_3(x, y, z, t) - \dot{z}(t - T)| \qquad \text{when} \quad e(t) < 0$$

When the trajectory close to our periodic orbit, the control signal is approach to zero. Fig. 3.46 show the phase portrait and Poincaré map for $K_1 = 0.03$.

(7) Controlling Chaos by External Force Control

A feedback control with a periodic external force of a special form is used in this method[17]. It is assumed that the input signal $u(t)$ disturbs only the third equation in (3.4.2).

and

$$u(t) = K_2[y_i(t) - y(t)] = K_2 D(t)$$

Here, $y(t)$ is the chaotic output signal, $y_i(t)$ is the periodic motion of system. The difference $D(t)$ between the signal $y_i(t)$ and $y(t)$ is used as a control signal. Here K_2 is an adjustable weight of the feedback. By selecting the weight K_2, we can convert chaotic behavior to periodic motion, the

bifurcation diagram is shown in Fig. 3.47. We can control the chaotic behavior to period-1 motion by choosing $K_2 = 0.9$. We also can convert the chaotic motion to period-2 and period-4 for a suitable K_2.

(8) Controlling Chaos by Optimal Control

Optimal control is a well-established engineering control strategy, and is useful for both linear and nonlinear system with linear or nonlinear controllers[6]. Now, we use a typical optimal control for a chaos control. We consider the equation(3.4.8) with a controller u and define the Hamilton function :

$$H(x, y, z, u, p) = \boldsymbol{p}^T \boldsymbol{F}(x, y, z, u, t) \quad , \quad \boldsymbol{p}^T = [p_1 \ p_2 \ p_3]$$

Following the variation principle of optimal control, we can obtain

$$p_1 y + p_2 [dz^2 \cos x + \frac{1}{2}(e + pz^2)\sin 2x - \sin x - by] = 0 \qquad (3.4.9)$$

$$- p_2(2dz \cos x + pz \sin 2x) = 0$$

$$(3.4.10)$$

This yield a non-trivial solution for (p_1, p_2) if and only if

$$2dz \cos x + pz \sin 2x = 0 \qquad (3.4.11)$$

It gives an optimal surface singularly in the state space. This type of control assumes values on the two allowable boundaries (3.4.9) alternatively according to a switching surface. Locating system trajectories on the surface, a typical feedback control in the form

$$u = -k_b \, \text{sgn}[2dz \cos x + pz \sin 2x]$$

can be used. By adjusting the value of k_b in the above controller with the signum function

$$\text{sgn}[v] = \begin{cases} 1 & \text{if} \quad v > 0 \\ 0 & \text{if} \quad v = 0 \\ -1 & \text{if} \quad v < 0 \end{cases}$$

the chaotic motion can be controlled to periodic motion which we desired by the bifurcation diagram as shown in Fig. 3.48.

3.4.3 Chaos Synchronization

Recall from Section 3.1.4, a natural way to develop synchronization for chaotic systems is through system decomposition. The coupled systems are decomposed into two subsystem as follows :

$$\begin{cases} \dot{x}_1 = y_1 \\ \dot{y}_1 = dz_1{}^2 \cos x_1 + \frac{1}{2}(e + pz_1{}^2)\sin 2x_1 - \sin x_1 - by_1 \\ \dot{z}_1 = q\cos x_1 - F - a\sin \overline{\omega}t \end{cases} \quad \text{(drive) (3.4.12)}$$

$$\begin{cases} \dot{x}_2 = y_2 \\ \dot{y}_2 = dz_2{}^2 \cos x_2 + \frac{1}{2}(e + pz_2{}^2)\sin 2x_2 - \sin x_2 - by_2 \\ \dot{z}_2 = q\cos x_2 - F - a\sin \overline{\omega}t \end{cases} \quad \text{(response) (3.4.13)}$$

By linear feedback approach, the error between the output of the identical drive and response is used as the control signal. The first equation of response(3.4.13) is combined with a linear feedback, while the equations of drive remain the same.

$$\begin{cases} \dot{x}_2 = y_2 + k(x_1 - x_2) \\ \dot{y}_2 = dz_2{}^2 \cos x_2 + \frac{1}{2}(e + pz_2{}^2)\sin 2x_2 - \sin x_2 - by_2 \\ \dot{z}_2 = q\cos x_2 - F - a\sin \overline{\omega}t \end{cases} \quad \text{(3.4.14)}$$

where k is the constant feedback gain. Complete synchronization between the two chaotic systems can be observed with k= 0.2, the trajectories of the

synchronization errors, $e_x = x_2 - x_1$, $e_y = y_2 - y_1$, and $e_z = z_2 - z_1$, are shown

in Fig. 3.49.

Chapter 2

The Analytical Analysis of the System
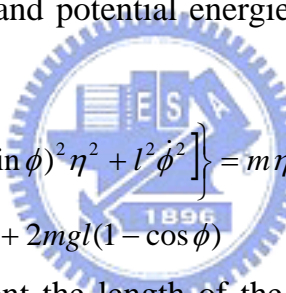
2.1 Equations of Motion

The rotational machine with centrifugal governor is depicted in Fig. 2.1. Some basic assumptions for the system are

(1) neglecting the mass of the rods and the sleeve;

(2) viscous damping in rod bearing of the fly-ball is presented by damping constant c.

From Fig. 2.1., the kinetic and potential energies of the system are written as follows:

$$T = 2 \times \left\{ \frac{1}{2} m \left[(r + l \sin \phi)^2 \eta^2 + l^2 \dot{\phi}^2 \right] \right\} = m\eta^2 (r + l \sin \phi)^2 + ml^2 \dot{\phi}^2$$

$$V = 2kl^2 (1 - \cos \phi)^2 + 2mgl(1 - \cos \phi)$$

where l, m, r and ϕ represent the length of the rod, the mass of fly ball, the distance between the rotational axis and the suspension joint, and the angle between the rotational axis and the rod. It is easy to obtain the Lagrangian

$$L = T - V = m\eta^2 (r + l \sin \phi)^2 + ml^2 \dot{\phi}^2 - 2kl^2 (1 - \cos \phi)^2 - 2mgl(1 - \cos \phi)$$

Then using Lagrange equation, the equation of motion for the governor can be derived as follows:

$$2[ml^2 \ddot{\phi} - mrl\eta^2 \cos \phi - (2k + m\eta^2)l^2 \sin \phi \cos \phi$$

$$+ (2kl + mg)l \sin \phi] = -c\dot{\phi} \tag{2.1}$$

where c is the damping coefficient.

For the rotational machine the net torque is the difference between the

torque Q produced by the engine and the load torque Q_L, which is available for angular acceleration. That is,

$$J \frac{d\omega}{dt} = Q - Q_L,$$ (2.2)

where J is the moment of inertia of the machine. As the angle ϕ varies, the position of control valve which admits the fuel is also varied. The dynamical equation (2.2) can be written in the form

$$J \dot{\omega} = \gamma \cos\phi - \beta$$ (2.3)

where $\gamma > 0$ is a proportionality constant and β is an equivalent torque of the load[13]. Equation (2.3) is the second differential equation of motion for the system.

Usually, the governor is geared directly to the output shaft such that its speed of rotation is proportional to the engine speed, i.e. $\eta = n\omega$. The operation of the fly-ball governor can be briefly described as follows. At first, set the speed of engine at ω_0. If the speed of engine drops down, the centrifugal force acting on the fly-ball would decrease, thus the control valve of fuel will open wider. When more fuel is supplied, the speed of the engine increases until equilibrium is again reached. Similarly, if the speed rises up, the fuel supply is reduced and the speed decreases until ω_0 is recovered.

Change time scale $\tau = \Omega_n t$, equation (2.1) and equation (2.3) can be written in nondimensional form

$$\dot{\phi} = \varphi$$
$$\dot{\varphi} = d\omega^2 \cos\phi + (e + p\omega^2)\sin\phi\cos\phi - \sin\phi - b\varphi$$ (2.4)
$$\dot{\omega} = q\cos\phi - F$$

where

$$q = \frac{\gamma}{J\Omega_n}, \; F = \frac{\beta}{J\Omega_n}, \; d = \frac{n^2 mr}{2kl + mg}, \; e = \frac{2kl}{2kl + mg}$$

$$p = \frac{n^2 ml}{2kl + mg}, \; b = \frac{c}{2ml^2\Omega_n}, \; \Omega_n = \sqrt{\frac{2kl + mg}{ml}},$$

and the dot presented the derivative with respect to τ, φ is $\frac{d\phi}{d\tau}$. Hence, the dynamics of the system of rotational machine with fly-ball governor is described by a three-dimensional autonomous system.

2.2 Stability Analysis by Lyapunov Direct Method

Find the equilibrium points of the system and determine the stability of them. These equilibrium points can be found from equation (2.4) as $p_e = (\phi_0, 0, \omega_0)$ with

$$\cos\phi_0 = \frac{F}{q}, \; \omega_0^2 = \frac{(q - eF)\sqrt{q^2 - F^2}}{F(dq + p\sqrt{q^2 - F^2})}$$

Add slightly disturbances x, y, z to the equilibrium point $(\phi_0, 0, \omega_0)$

$$\phi = \phi_0 + x, \varphi = y, \; \omega = \omega_0 + z \tag{2.5}$$

Substituting equation (2.5) into equation (2.4), and expanding to Taylor series, it becomes

$$\dot{x} = y$$

$$\dot{y} = -Ax - By + Cz + \cdots \tag{2.6}$$

$$\dot{z} = -Dx + \cdots$$

where

$$A = \{\omega_0^2[dq\sqrt{q^2 - F^2} - p(2F^2 - q^2)] + qF - e(2F^2 - q^2)\}/q^2$$

$$B = b,$$

$$C = 2\omega_0 F(dq + p\sqrt{q^2 - F^2})/q,$$

$$D = \sqrt{q^2 - F^2}.$$

and the terms higher than one degree have not been written down. Let $q > F > 0$, then $A > 0$, $B > 0$, $C > 0$ and $D > 0$.

First, asymptotical stability of the origin of equation (2.6) can be studied by using Lyapunov direct method. Construct the quadratic Lyapunov function candidate in the form

$$V(x, y, z) = A_{11}x^2 + A_{22}y^2 + A_{33}z^2 + 2A_{12}xy + 2A_{13}xz - 2yz.$$

Let p_i $(i = 1,2,3)$ be the principal minor determinants of the characteristic matrix of the quadratic form, then

$$p_1 = A_{11}$$

$$p_2 = A_{11}A_{22} - A_{12}^2$$

$$p_3 = A_{11}A_{22}A_{33} - 2A_{12}A_{13} - A_{11} - A_{22}A_{13}^2 - A_{33}A_{12}^2$$
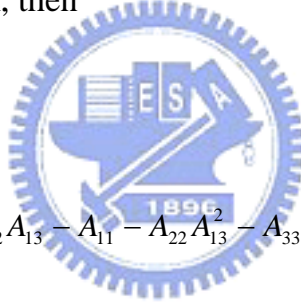
By Sylvester's criterion [14], V is positive definite if and if that all p_i are positive:

$$A_{11} > 0$$

$$A_{11}A_{22} - A_{12}^2 > 0$$

$$A_{11}A_{22}A_{33} - 2A_{12}A_{13} - A_{11} - A_{22}A_{13}^2 - A_{33}A_{12}^2 > 0$$

The derivative of V with respect to τ is given by

$$\dot{V} = -2(AA_{12} + DA_{13})x^2 + (2A_{12} - 2CA_{22})y^2 - 2Bz^2 + (2A_{11} - 2AA_{22} - 2CA_{12} + 2D)xy + (2A + 2BA_{12} - 2DA_{33})xz + (2C + 2A_{13} + 2BA_{22})yz + \cdots$$

Now, it is necessary to choose A_{11}, A_{22}, A_{33}, A_{12} and A_{13} such that V and $-\dot{V}$ are positive definite. Let

$$A_{11} = \frac{AC + A^2C + B^2C + BC^2D + B^3D + CD^2}{AB - CD}$$

$$A_{22} = \frac{C + AC + BD}{AB - CD}$$

$$A_{33} = \frac{A^2B + BC^2 - ACD + C^3D + B^2CD}{ABD - CD^2}$$

$$A_{12} = \frac{BC + B^2D + C^2D}{AB - CD}$$

$$A_{13} = \frac{C^2 + AB^2 + AC^2}{CD - AB}$$

Then

$$\dot{V}(x, y, z) = -B(x^2 + y^2 + z^2) + \cdots$$

is negative definite. By Sylvester's theorem, the sufficient condition for V be positive definite is founded:

$$AB > CD$$

i.e.,

$$b > \frac{2qF[d\sqrt{q^2 - F^2} + p(q^2 - F^2)]}{\omega_0[d\sqrt{q^2 - F^2} - p(2F^2 - q^2)] + qF - e(2F^2 - q^2)} \tag{2.7}$$

From the Lyapunov asymptotic stability theorem, we conclude that the origin is asymptotically stable. Furthermore, the result is the same as analysis by linearized system.

For the given range for disturbance　, we can find the allowable range for the initial disturbances 　 by the Lyapunov function. Let

$$R^2 = x^2 + y^2 + z^2$$

Using the method of Lagrange's multiplier, we form the Lagrange's function $L = R^2 + \lambda V$. From

$$\frac{\partial L}{\partial x} = 0 , \frac{\partial L}{\partial y} = 0 , \frac{\partial L}{\partial z} = 0$$

we have

$$\lambda_1 = \frac{-u_2}{3u_3} - \frac{\sqrt[3]{2}(-u_2^2 + 3u_1u_3)}{(-2u_2^3 + 9u_1u_2u_3 - 27u_3^2 + \sqrt{4(-u_2^2 + 3u_1u_3)^3 + (-2u_2^3 + 9u_1u_2u_3 - 27u_3^2)^2})^{\frac{1}{3}}}$$

$$+ \frac{(-2u_2^3 + 9u_1u_2u_3 - 27u_3^2 + \sqrt{4(-u_2^2 + 3u_1u_3)^3 + (-2u_2^3 + 9u_1u_2u_3 - 27u_3^2)^2})^{\frac{1}{3}}}{3 \times \sqrt[3]{2}u_3}$$

$$\lambda_{2,3} = \frac{-u_2}{3u_3} + \frac{(1 \pm \sqrt{3}i)(-u_2^2 + 3u_1u_3)}{(-2u_2^3 + 9u_1u_2u_3 - 27u_3^2 + \sqrt{4(-u_2^2 + 3u_1u_3)^3 + (-2u_2^3 + 9u_1u_2u_3 - 27u_3^2)^2})^{\frac{1}{3}}}$$

$$- \frac{(1 \mp \sqrt{3}i)(-2u_2^3 + 9u_1u_2u_3 - 27u_3^2 + \sqrt{4(-u_2^2 + 3u_1u_3)^3 + (-2u_2^3 + 9u_1u_2u_3 - 27u_3^2)^2})^{\frac{1}{3}}}{6 \times \sqrt[3]{2}u_3}$$

where

$$u_1 = A_{11} + A_{22} + A_{33}$$
$$u_2 = -1 + A_{11}A_{22} + A_{11}A_{33} + A_{22}A_{33} - A_{12}^2 - A_{13}^2$$
$$u_3 = -A_{11} + A_{11}A_{22}A_{33} - A_{33}A_{12}^2 - 2A_{12}A_{13} - A_{22}A_{13}^2$$

When $\lambda = \lambda_1$, we have

$$x = x, \ y = z = 0$$

Putting these in $V = c$, we have $x = x(c) = \pm\sqrt{c/A_{11}}$. Similarly, for $\lambda_{2,3}$ we have $x = x(c)$, $y = y(c)$, $z = z(c)$. Putting all these solutions in R^2, we obtain $R_x^2(c)$, $R_y^2(c)$, $R_z^2(c)$, of which the minimum is

$$R_{\min}^2(c) = \min\{R_x^2(c), R_y^2(c), R_z^2(c)\}$$

Taking $\varepsilon = R_{\min}^2(c)$, we have the inverse function $c = R_{\min}^2{}^{-1}(\varepsilon)$. Let $\Omega = \frac{R_{\min}}{\sqrt{3}}$, then $V = c$ is outside of the hypersurface $\max\{|x|, |y|, |z|\} = \Omega$. So we have, for given ε,

$$\Omega = \frac{R_{\min}}{\sqrt{3}}$$

Next, the stability of the fixed point $(\phi_0, 0, -\omega_0)$ is studied. The

differential equations for disturbances are

$$\dot{x} = y,$$
$$\dot{y} = -Ax - By - Cz + \cdots,$$
$$\dot{z} = -Dx + \cdots,$$

(2.8)

where A, B, C, D are the same as above.

In order to determine the instability of the origin of equation(2.8), the quadratic Lyapunov function candidate is assumed in the form

$$V(x, y, z) = -(A + D)x^2 - y^2 + \frac{A}{D}z^2 - (B + C)xz - yz.$$

The derivative of V with respect to τ along the trajectories of system is given by

$$\dot{V} = 2(BD + CD)x^2 + 2Cy^2 + 2Bz^2 + \cdots$$

which is positive definite. There exists the region $V(x, y, z) > 0$ in the neighborhood of the origin of equation(2.2.8). Its boundaries in the y-z plane are

$$y = \frac{-D + \sqrt{AD + D^2}}{D} z \quad \text{or} \quad y = \frac{-D - \sqrt{AD + D^2}}{D} z.$$

in the x-z plane are

$$x = \frac{-(B + C)D + \sqrt{(B + C)^2 D^2 + AD(A + D)}}{D(A + D)} z$$

or

$$x = \frac{-(B + C)D - \sqrt{(B + C)^2 D^2 + AD(A + D)}}{D(A + D)} z.$$

So, by the Lyapunov instability theorem, the origin is unstable.

Chapter 4

Conclusions

The dynamic system of the rotational machine with a hexagonal centrifugal governor exhibits a rich variety of nonlinear behaviors as certain parameters are varied. Due to the effect of nonlinearity, regular or chaotic motions may occur. In this thesis, both analytical and computational methods have been employed to study the dynamical behaviors of the nonlinear system. The conditions of stability and instability of fixed points have been determined by using the Lyapunov direct method in Chapter 2.

The computational analyses have been studied in Chapter 3. For autonomous system, the periodic and chaotic motions of the autonomous system have been obtained by the numerical methods such as phase trajectory, power spectrum, Poincaré map and Lyapunov exponents. The changes of parameters play a major role for the nonlinear system. The chaotic motion has been detected by using Lyapunov exponents and Lyapunov dimensions. In spite of that these methods are different, the results obtained matches each other. In order to improve the performance of a dynamical system or avoid the chaotic phenomena, four methods: delayed feedback control, linear feedback control, optimal control and adaptive control algorithm are used to control the chaotic motion to any assigned periodic motion effectively. Especially, for our system, the delayed feedback control is the best method compared with the others, for which the control time is minimum and the delay time and the gain can be

easily selected. Synchronization of two chaotic oscillators is studied in this thesis. For coupled systems, increase of coupling strength leads to the occurrence of phase synchronization. We show that one of the zero Lyapunov exponents becoming negative cannot be used as a sufficient criterion for the occurrence of phase-locking synchronization. However, one of the negative Lyapunov exponents approaching zero gives a clue of the appearance of phase synchronization of a coupled system.

For anticontrol of chaos of autonomous system, two different procedures to design the controller have been presented. The periodic motion of the system is disappeared and replaced by chaotic motion effectively by adding a linear and a nonlinear feedback term, respectively. Chaos synchronization of the autonomous governor system has been presented by adding linear feedback term, adding sinusoidal term and adaptive feedback methods. Chaos synchronization is also attained by a recursive procedure, backstepping design that combines the choice of a Lyapunov function for selecting a proper controller. Besides, the parameter of chaotic system is estimated from time sequences for chaos synchronization has been studied.

In section 3.3, the periodic and chaotic motions of the autonomous system with time-delay have been obtained by the numerical methods such as phase trajectory, time history and power spectrum. In order to improve the performance of a dynamical system or avoid the chaotic phenomena, two methods, adaptive control algorithm and linear feedback control, are used to control the chaotic motion to periodic motion effectively. Synchronization of two chaotic oscillators is studied. For two chaotic systems, increase of coupling strength leads to the occurrence of completely synchronization and phase synchronization. Finally, anticontrol of chaos is also studied in this section.

The chaotic dynamics of the nonautonomous system have been obtained by the numerical methods such as power spectrum, Poincaré map and Lyapunov exponents in section 3.4. All these phenomena have been displayed in bifurcation diagrams. More information of the behaviors of the periodic and the chaotic motion can be found in parametric diagrams. Chaotic motion is the motion which has a sensitive dependence on initial condition in deterministic physical systems. The chaotic motion has been detected by using Lyapunov exponents and Lyapunov dimensions. The presence of chaotic behavior is generic for suitable nonlinearities, ranges of parameters and external force, where one wish to avoid or control so as to improve the performance of a dynamical system. Eight methods are used to control chaos effectively. Especially, we can control the chaotic motion to any assigned periodic motion by addition of period force, periodic impulse control, the delayed feedback control, external force feedback control, optimal control and adaptive control algorithm. For our system, the delayed feedback control is the best method compared with the others.

Reference

1. S. Wiggins 2003 *Introduction to Applied Nonlinear Dynamical Systems and Chaos*. New York: Springer-Verlag.

2. J. Guckenheimer and P. J. Holmes 1983 *Nonlinear Oscillations of Dynamical Systems and Bifurcations of Vector Fields*. New York: Springer-Verlag.

3. S. Wiggins 1988 *Global Bifurcations and Chaos.* New York: Springer-Verlag.

4. Z. M. Ge 2001 *Bifurcation, Chaos and Chaos Control of Mechanical Systems*. Gaulih Book Company, Taipei, Taiwan.

5. L. M. Pecora and T. L. Carroll 1990 *Physical Review Letter* **64**, 821-823. Synchronization in chaotic systems.

6. G. Chen and X. Dong 1998 *From Chaos to Order: Methodologies, Perspectives and Applications.* Singapore: World Scientific.

7. M. Lakshmannan and K. Murali 1996 *Chaos in Nonlinear Oscillators : Controlling and Synchronization.* World Scientific Pub., Singapore.

8. A. Pikovsky, M. Rosenblum and J. Kurths 2003 *Synchronization : A universal concept in nonlinear sciences*. University Press. Cambridge.

9. M. Rosenblum, A. Pikovsky, and J. Kurths 1996 *Physical Review Letters,* **76**, 1804-1807. Phase Synchronization of Chaotic Oscillators.

10. J. W. Shuai and D. M. Durand 1999 *Physics Letters A,* **264**, 289-297. Phase Synchronization in Two Coupled Chaotic Neurons.

11. G. Chen 1997 *IEEE* **2**, 181-186, Control and anticontrol of chaos.

12. G. Chen and X. Yu 2003 *Chaos Control : Theory and Applications*, New York: Springer-Verlag.

13. L. S. Pontryagin 1962 *Ordinary Differential Equations*. Addison-Wesley, Reading, Massachusetts.

14. H. K. Khalil 2002 *Nonlinear Systems* ,3rd ed. Prentice Hall.

15. A. Wolf, J. B. Swift, H. L. Swinney and J. A. Vastano 1985, *Physica, 16D*, Determining Lyapunov Exponents from a Time Series.

16. P. Frederickson, J. L. Kaplan, E. D. Yorke and J. A. Yorke 1983 *Journal of Differential Equations,* **49**, p.185-207. The Lyapunov Dimension of Strange Attractors.

17. K. Pyragas 1992 *Physics Letters A,* **170,** 421-428. Continuous Control of Chaos by Self-Controlling Feedback.

18. B. A. Huberman and E. Lumer 1990 *IEEE Transaction on Circuits and Systems*, **37**, 547-550. Dynamics of Adaptive System.

19. M. G. Rosenblum, A. S. Pikovsky and J. Kurths 1996 *Physical Review Letters,* **76**, 1804-1807. Phase Synchronization of Chaotic Oscillators.

20. Jian-Wei Shuai and Dominique M. Durand 1999, *Physics Letters A,* **264,** p.289-297. Phase Synchronization in Two Coupled Chaotic Neurons.

21. J. K. John and R. E. Amritkar 1994 *International Journal of Bifurcation and Chaos* **4**, 1687-1695. Synchronization by feedback and adaptive control.

22. C. W. Wu, T. Yang and L.O. Chua 1996 *International Journal of Bifurcation and Chaos* **6**, 455-471. On adaptive synchronization and control of non-linear dynamical systems.

23. X. Tan, J. Zhang and Y. Yang 2003 *Chaos, Solitons and Fractals* **16**, 37-45. Synchronization chaotic systems using backstepping design.

24. H. Sakaguchi 2002 *Physical Review E* **65**, 027201. Parameter evaluation from time sequences using chaos synchronization.
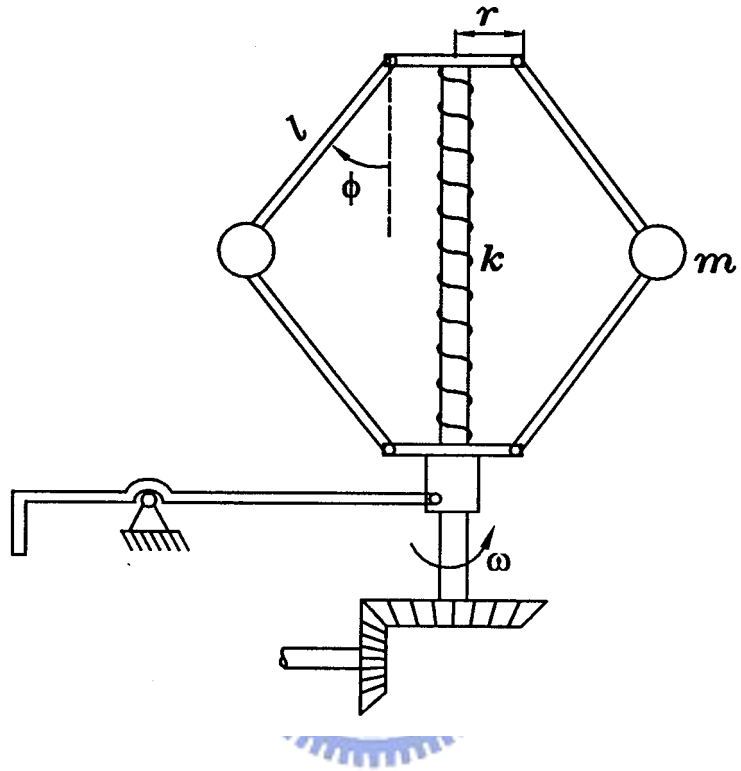
Fig. 2.1. Physical model of the system
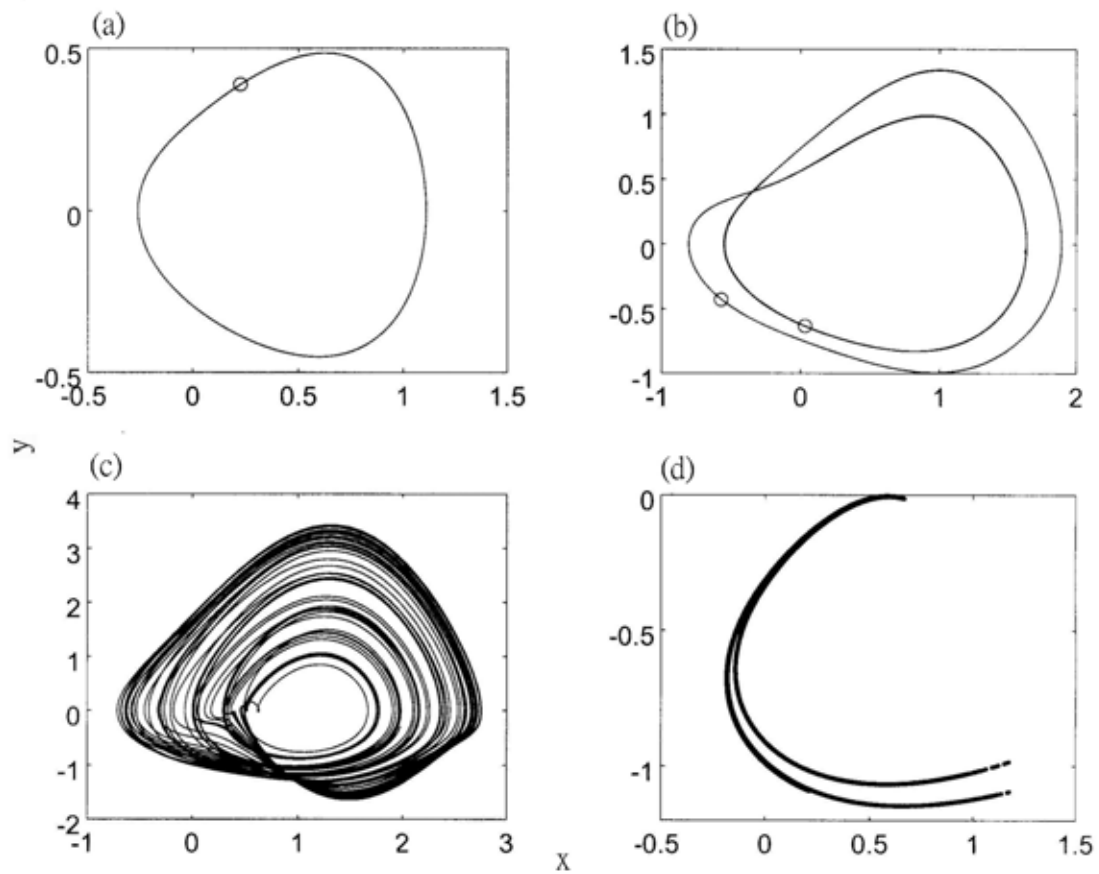
Fig. 3.1. (a) Phase portrait and Poincaré map for q=2.3 (b) q=3 (c) phase portrait for q=5.5 (d) Poincaré map for q=5.5
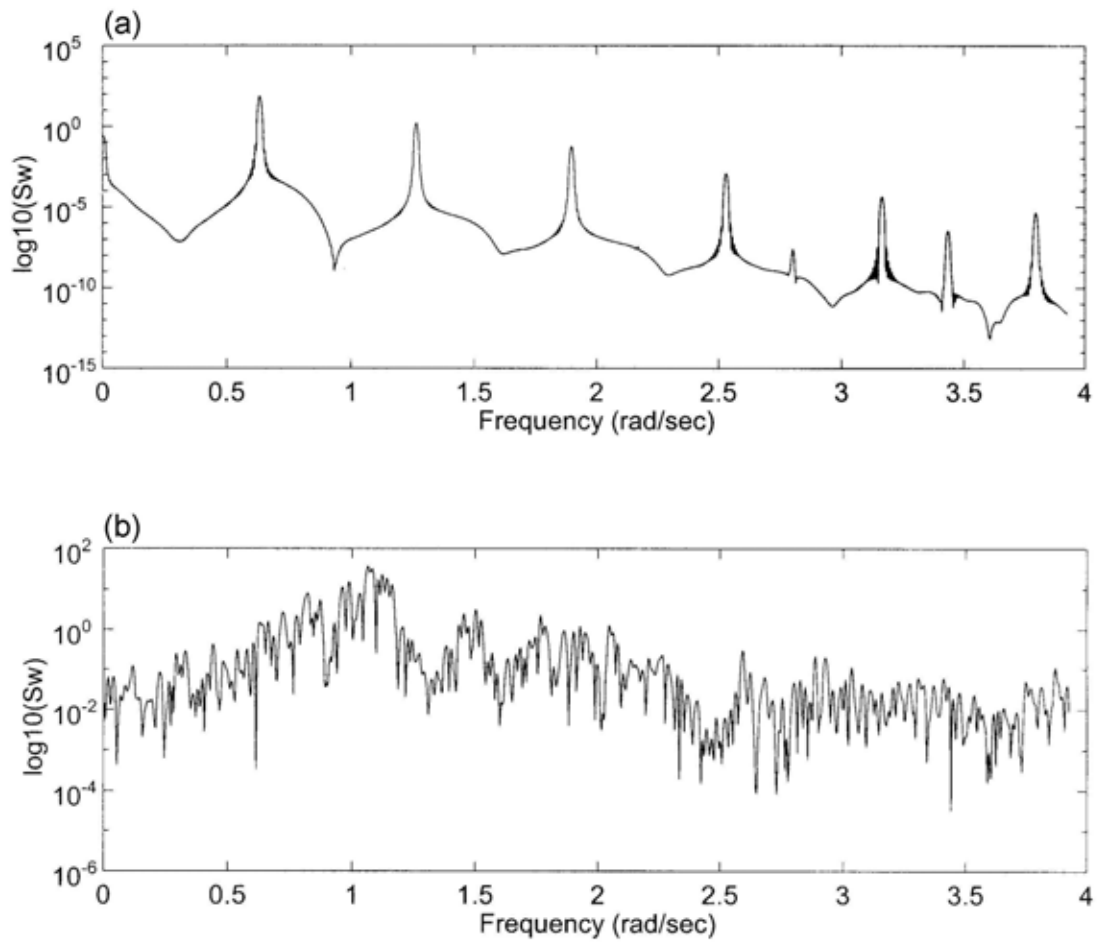
Fig. 3.2 (a) Power spectrum for *q*=2.3 (b) *q*=5.5
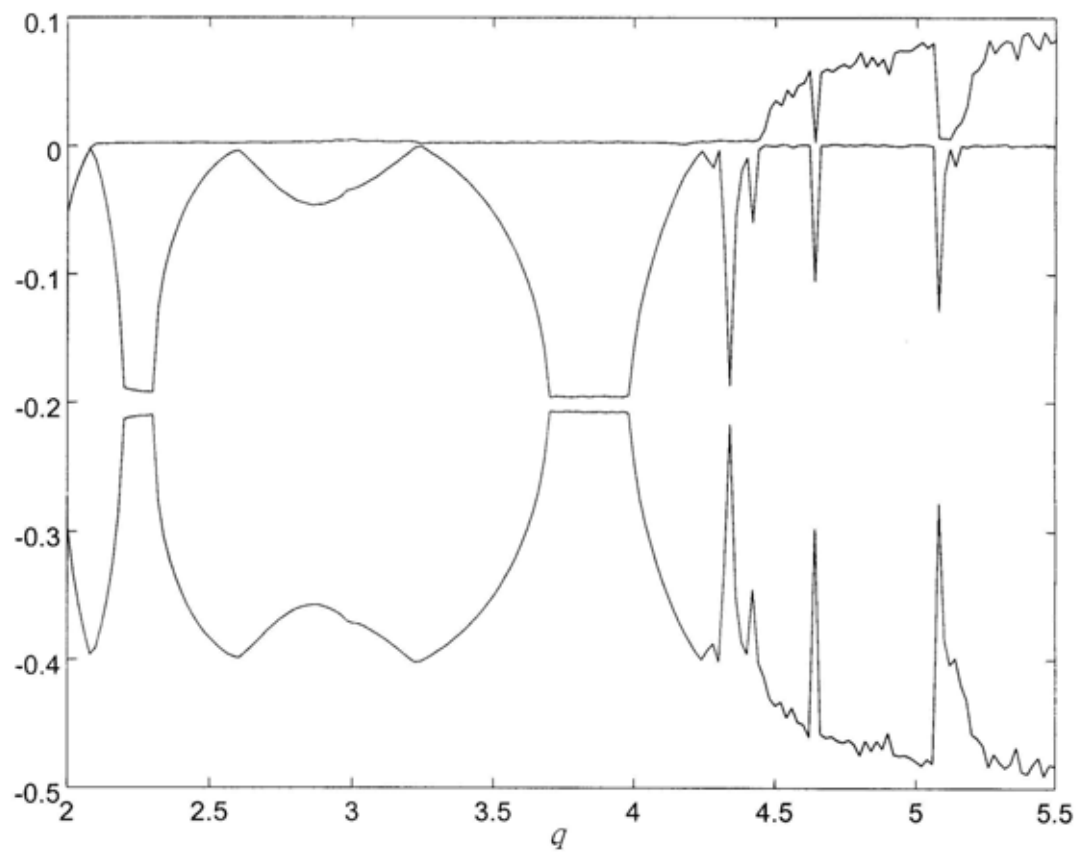
Fig. 3.3. The Lyapunov exponents for *q* between 2.3 and 5.5
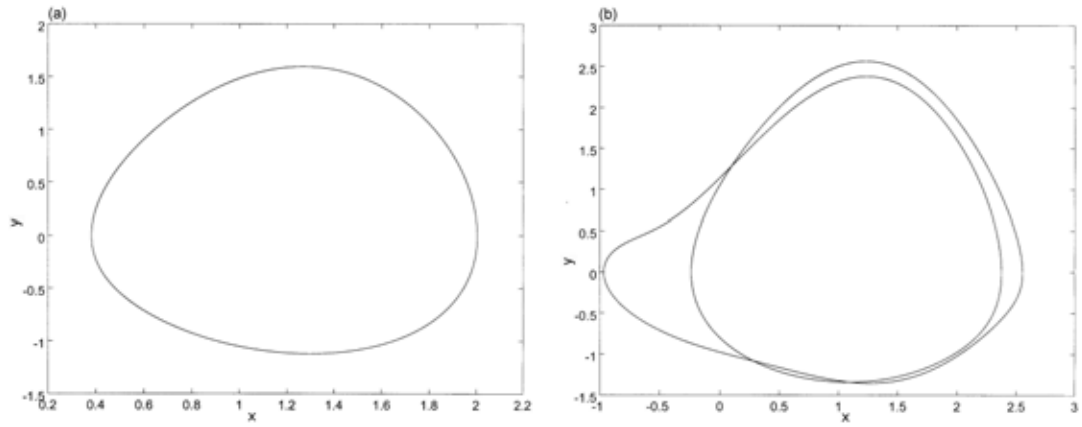
Fig. 3.4. Phase portrait of controlled system (a) $\tau = 5$, (b) $\tau = 4$
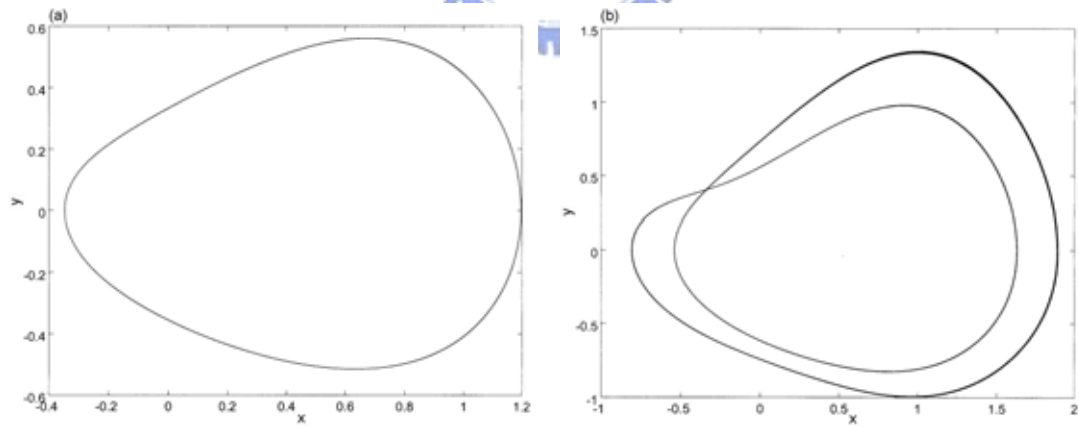
Fig. 3.5. Phase portrait of controlled system via adaptive feedback control
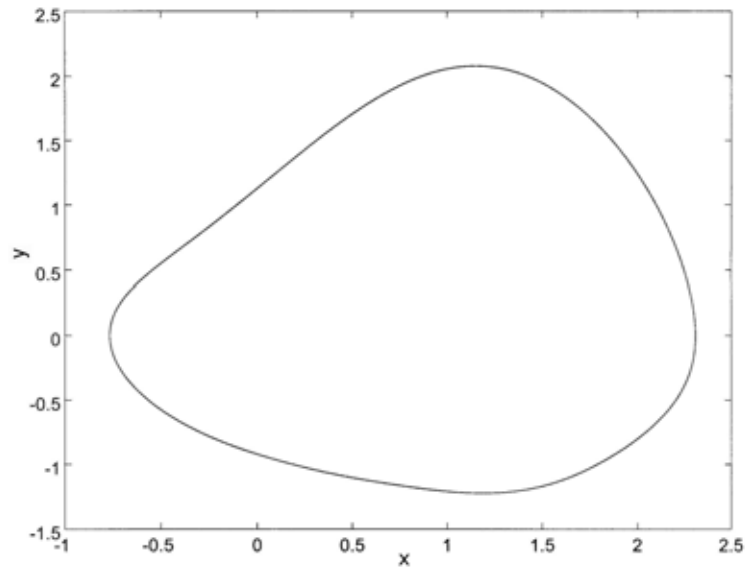
Fig. 3.6. Phase portrait of controlled system via linear feedback control
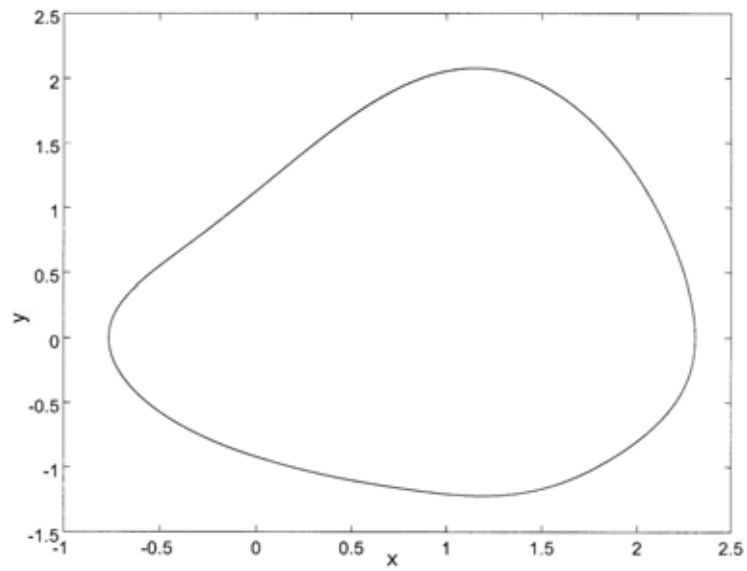
Fig. 3.7. Phase portrait of controlled system via optimal control
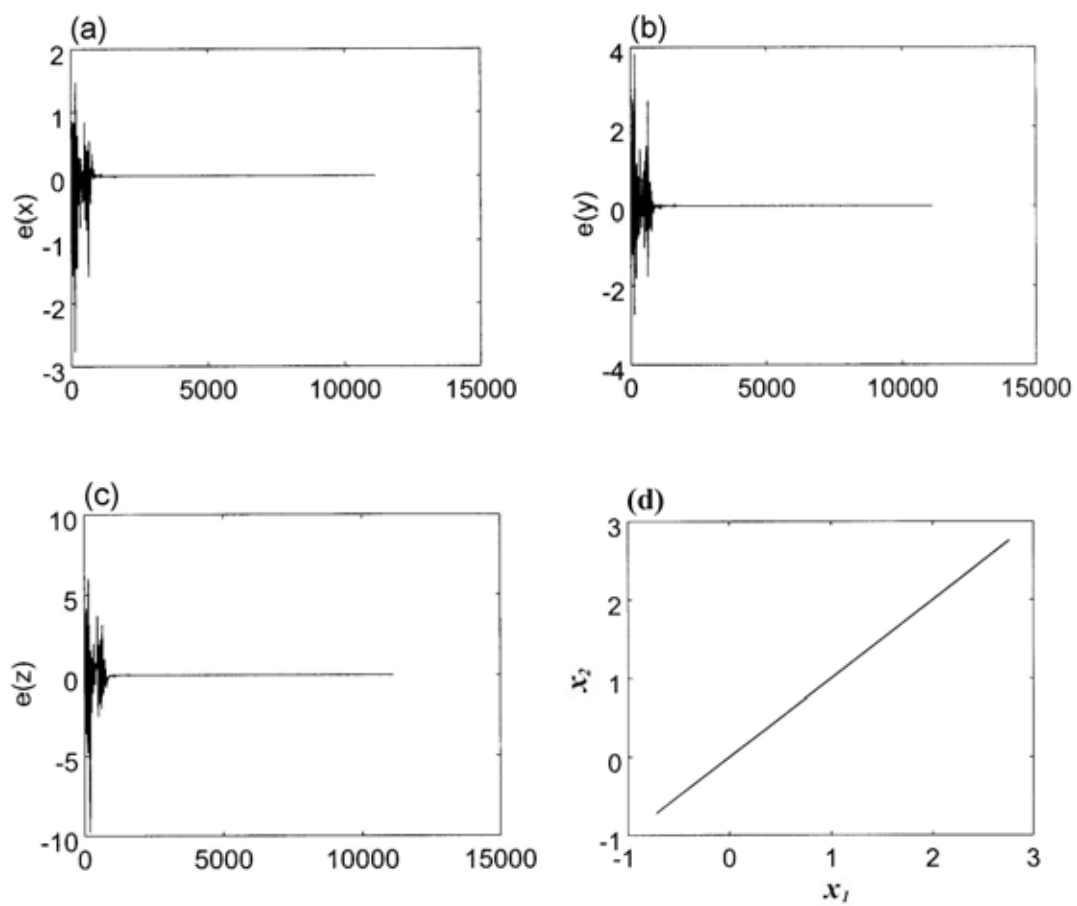
Fig. 3.8 Chaos synchronization via a linear feedback approach
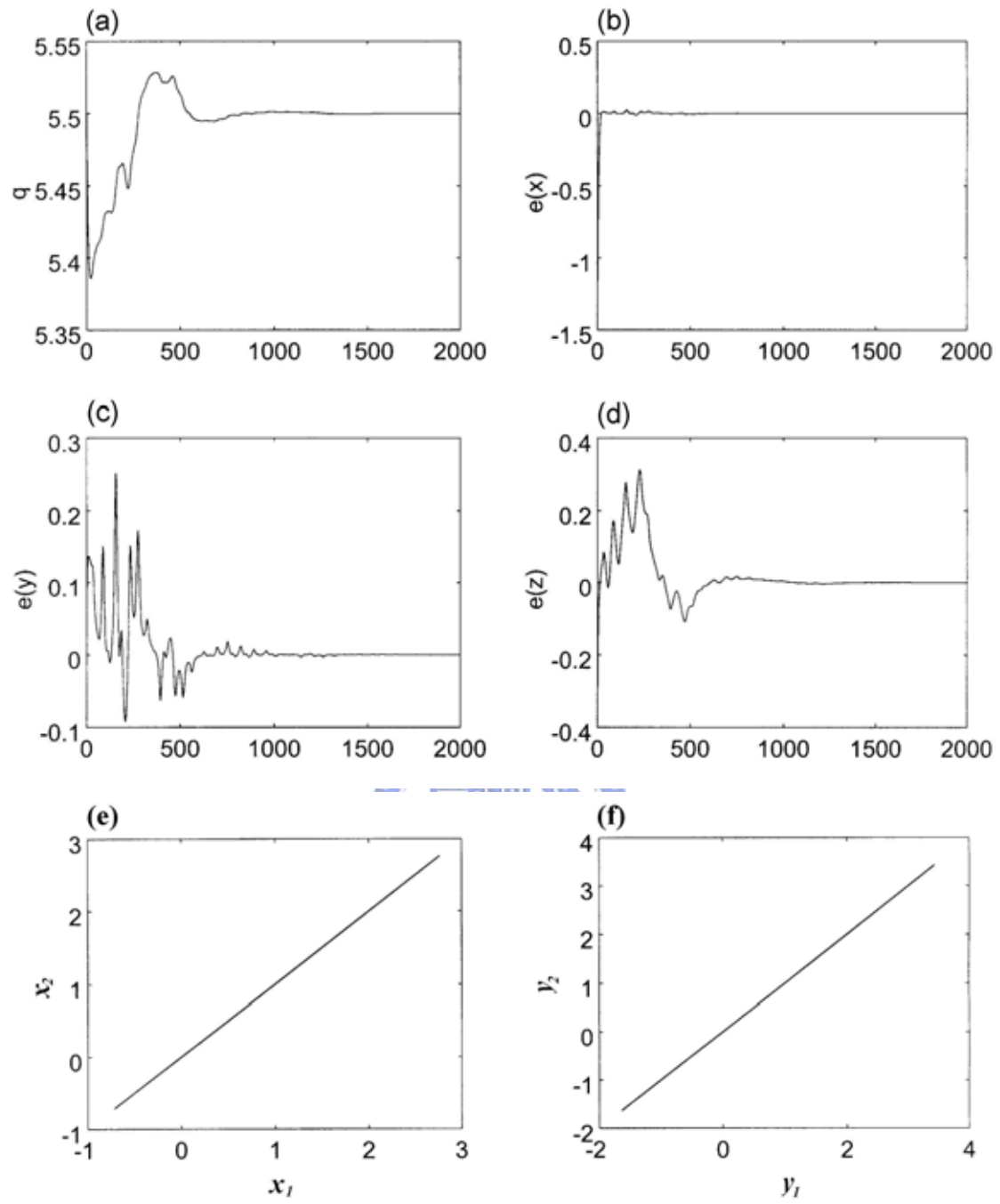
Fig. 3.9. Chaos synchronization via adaptive feedback with $k_1=10$ and $k_2=1$
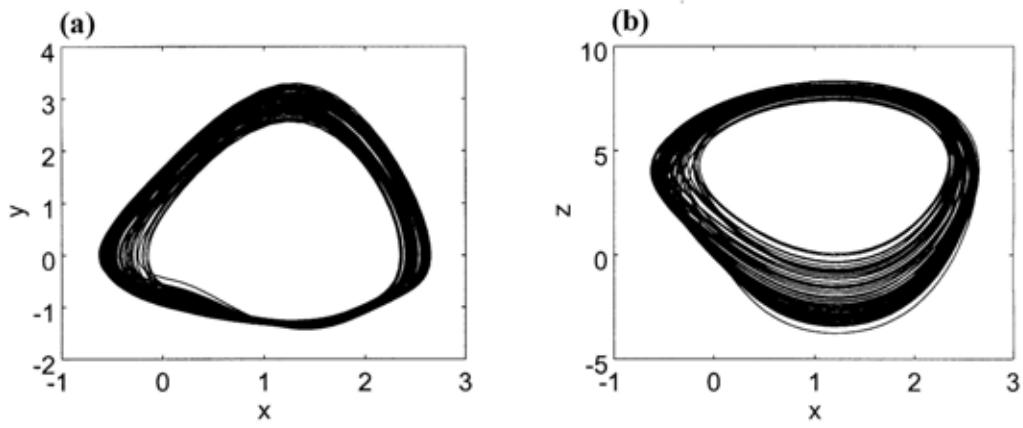
Fig. 3.10. The projection of the attractor in the x-y plane(a) and x-z plane(b) with the coupling strength $K = 0.1$.
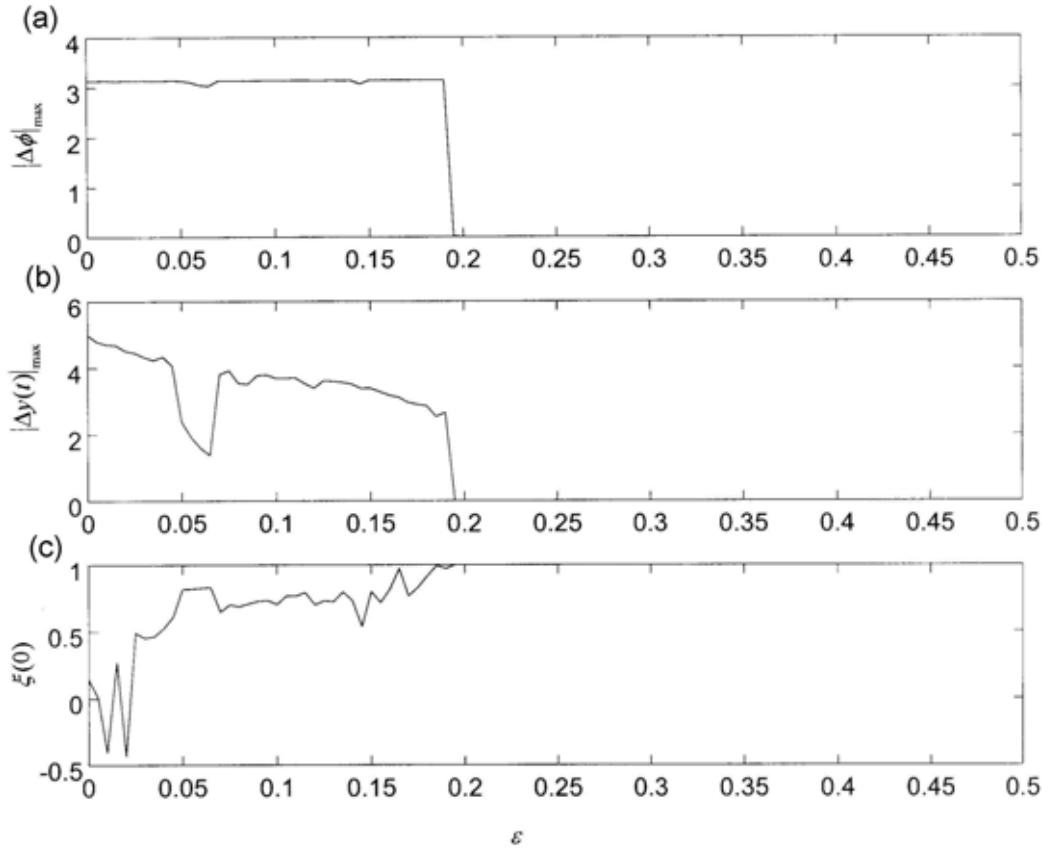
Fig. 3.11. (a) shows the maximum absolute difference of two phases. (b) shows the maximum absolute difference of two trajectories. (c) The cross-correlation function $\xi(0)$ with $\tau = 0$
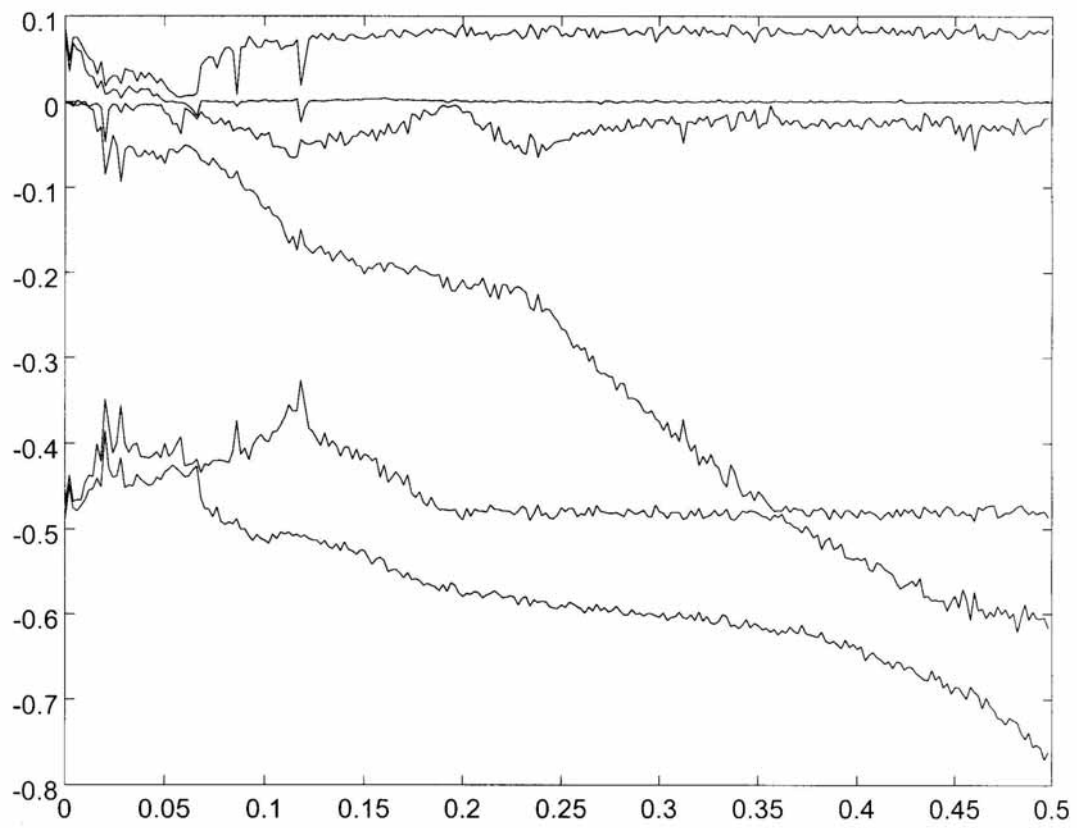
Fig. 3.12. The Lyapunov exponents of coupled system.
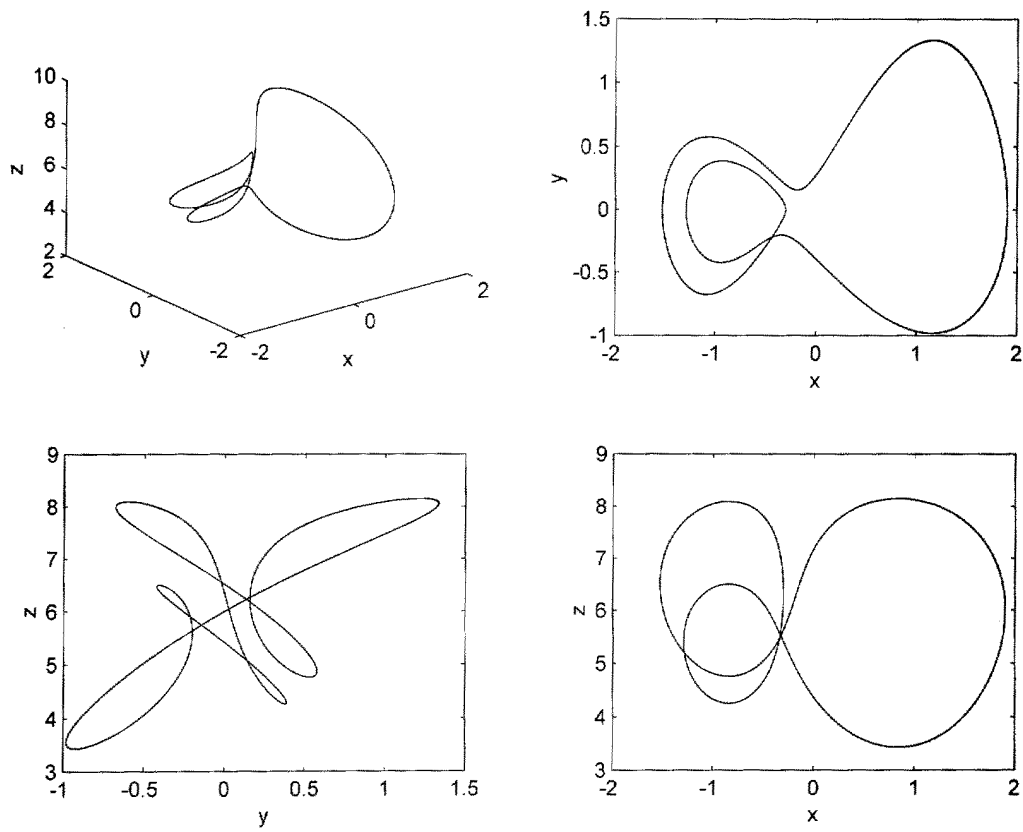
Fig. 3.13. Phase portrait of uncontrolled system ($a_1 = a_2 = a_3 = 0$).
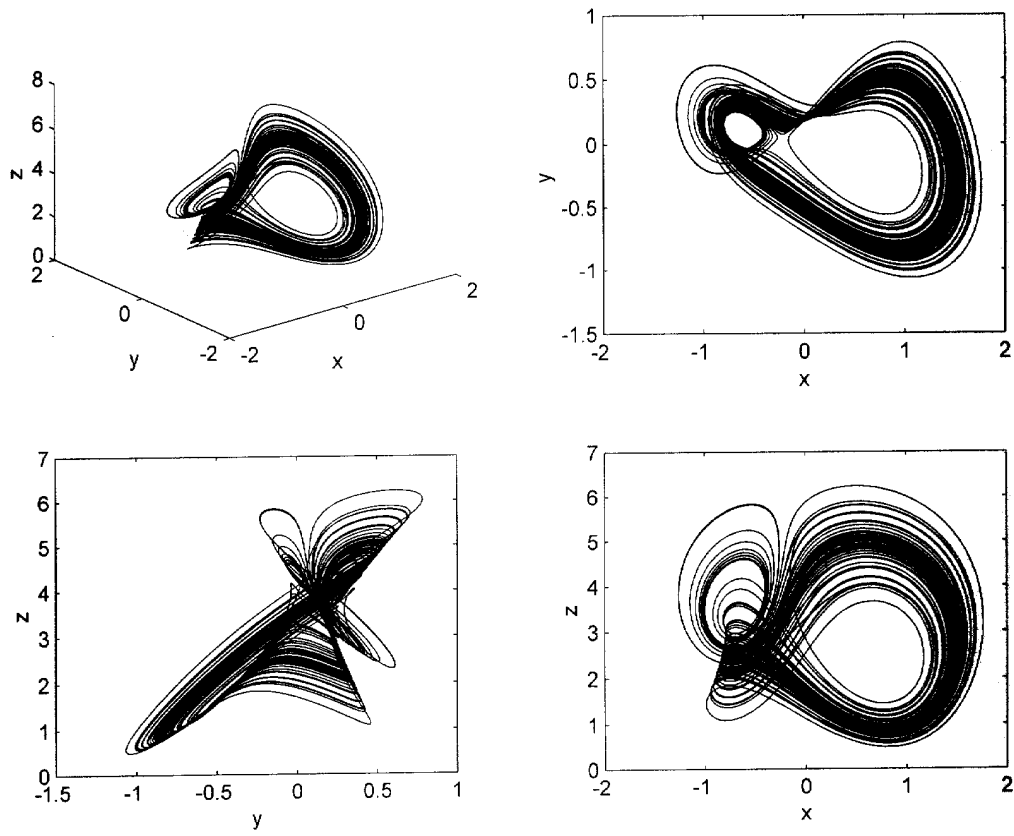
Fig. 3.14 Phase portrait of controlled system with $a_1 = 0.2, a_2 = -0.1, a_3 = -0.1$.

(a)

(b)
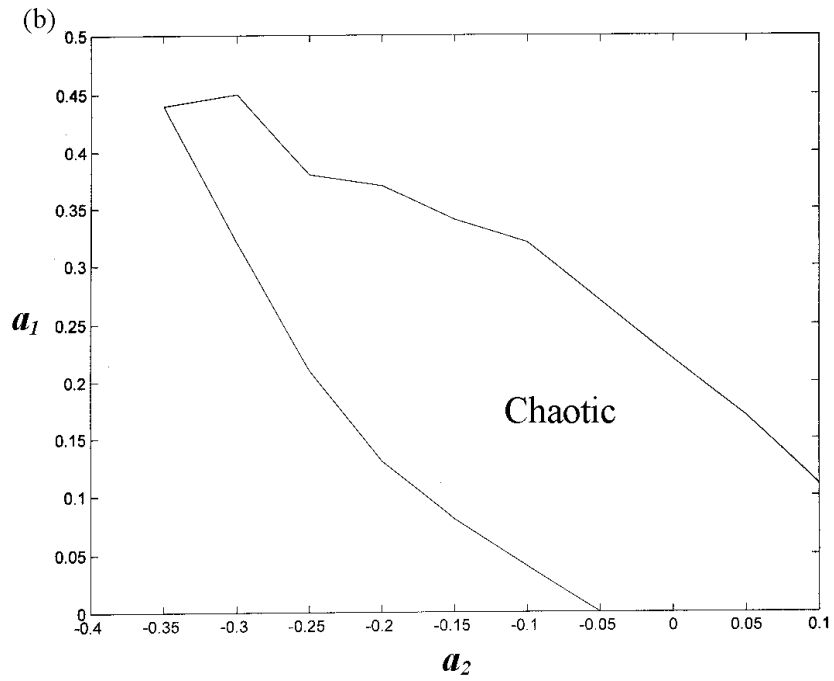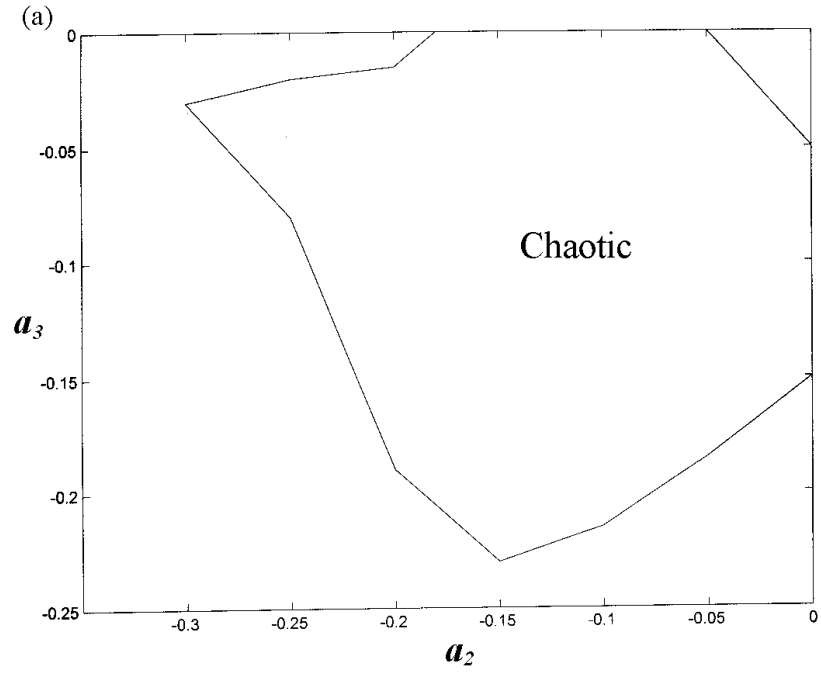
Fig. 3.15. parameter diagram of (a) a_2 versus a_3 for $a_1 = 0.2$, (b) a_2 versus a_1 for $a_3 = -0.1$.
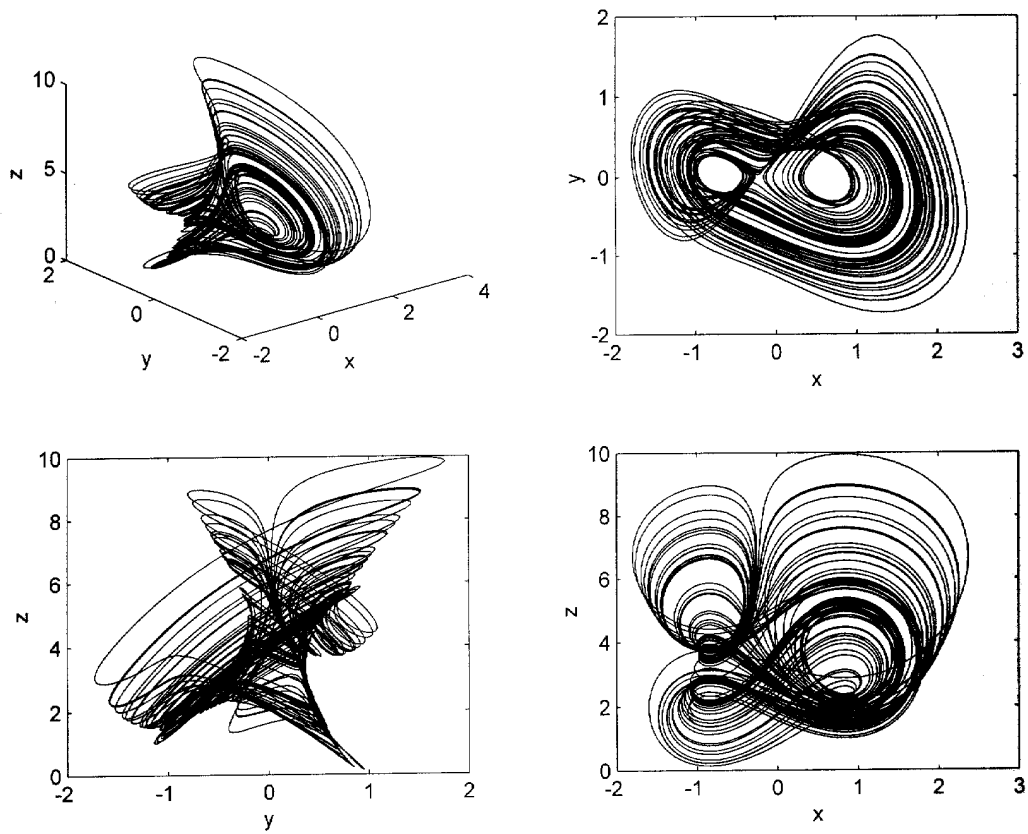
Fig. 3.16 Phase portrait of controlled system with $\varepsilon = 0.01$.
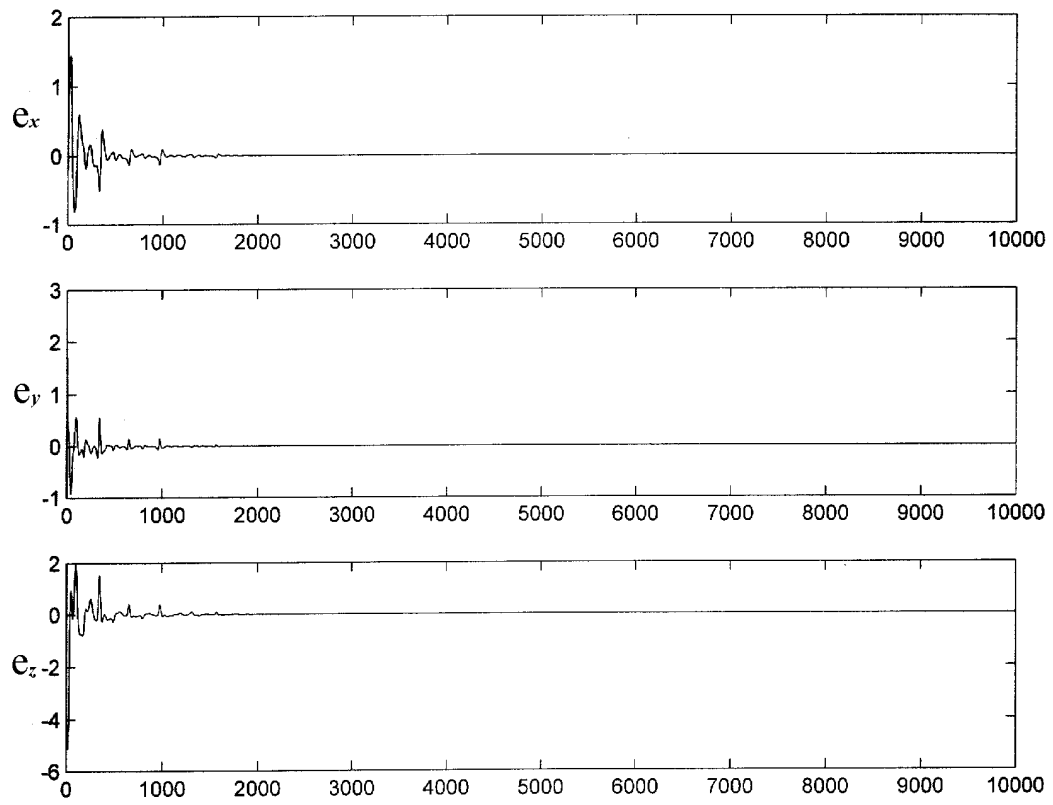
Fig. 3.17. Chaos synchronization via a linear feedback with $k_1 = 0.2$.
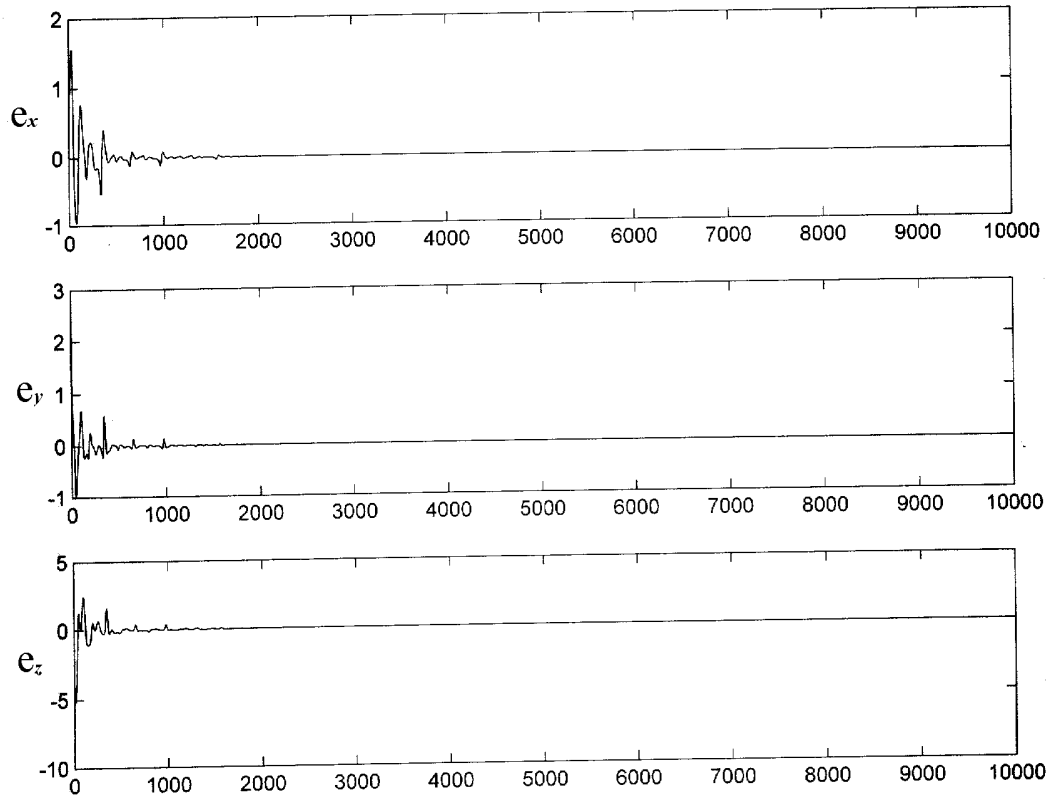
Fig. 3.18. Chaos synchronization via a nonlinear feedback with $k_2 = 0.2$.
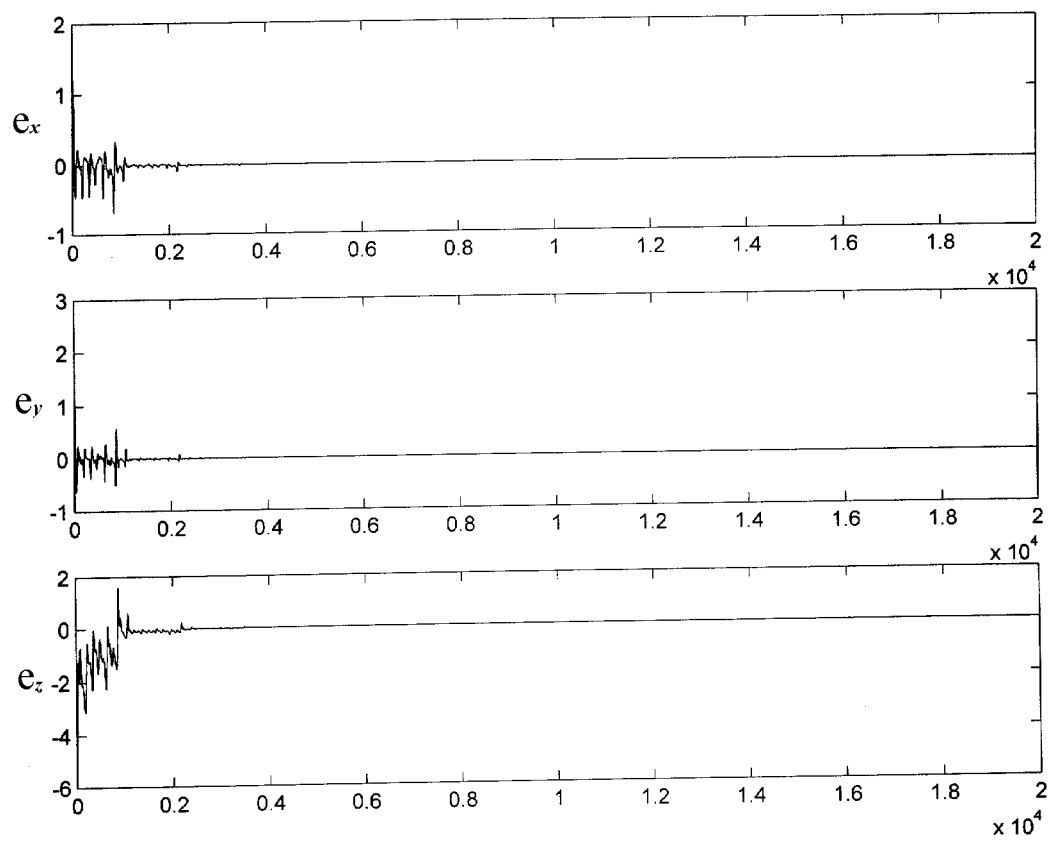
Fig. 3.19. Chaos synchronization via adaptive feedback with k_3=0.5 and k_4=0.2.
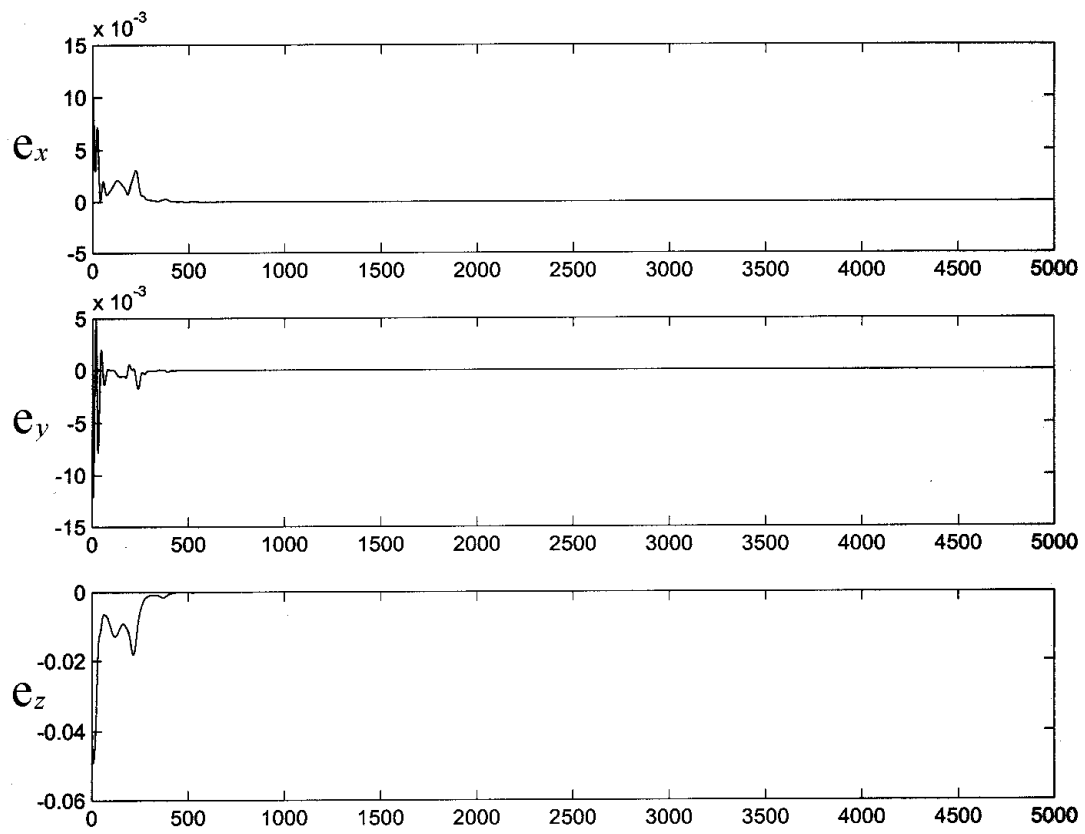
Fig. 3.20. Chaos synchronization via backstepping design.
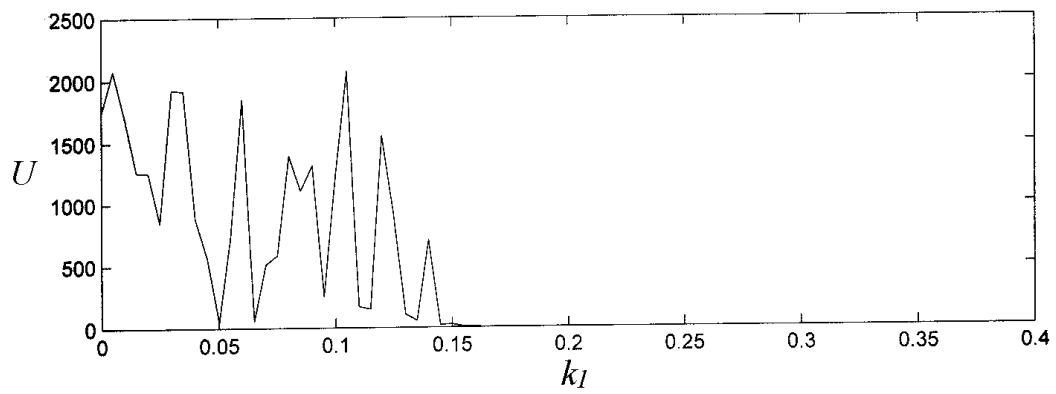
Fig. 3.21. The minimum value of U with respect to the coupling constant k_1
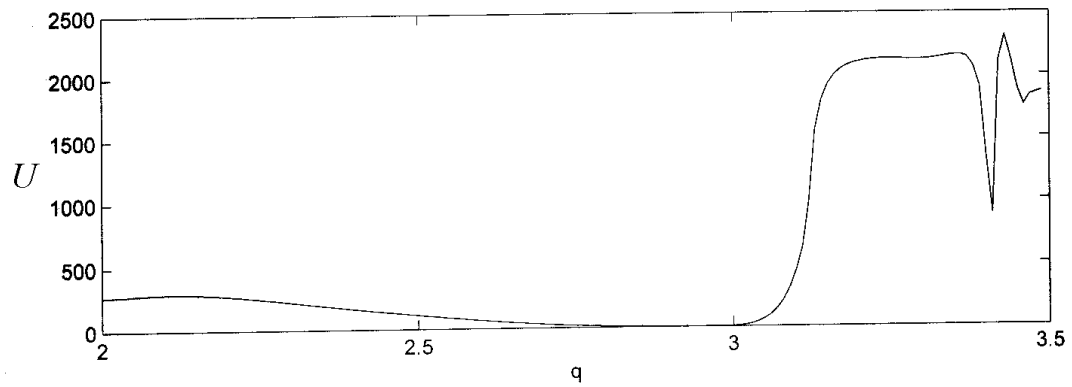
Fig. 3.22. The difference U versus the parameter q for $k_1 = 0.2$.
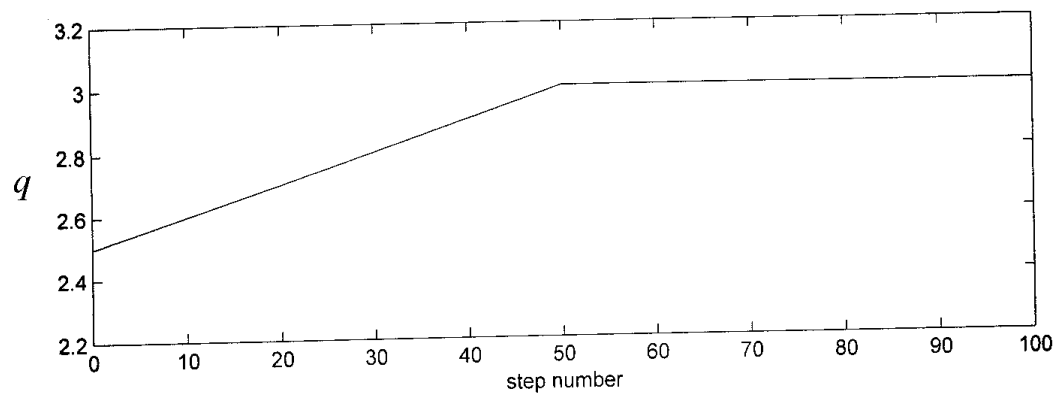
Fig. 3.23. Time evolution of the parameter q by the random optimization process.
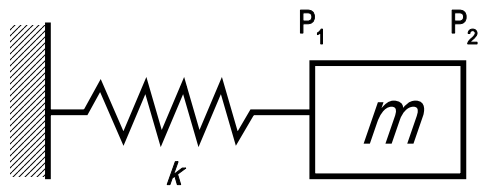
Fig. 3.24. A mass-spring system.
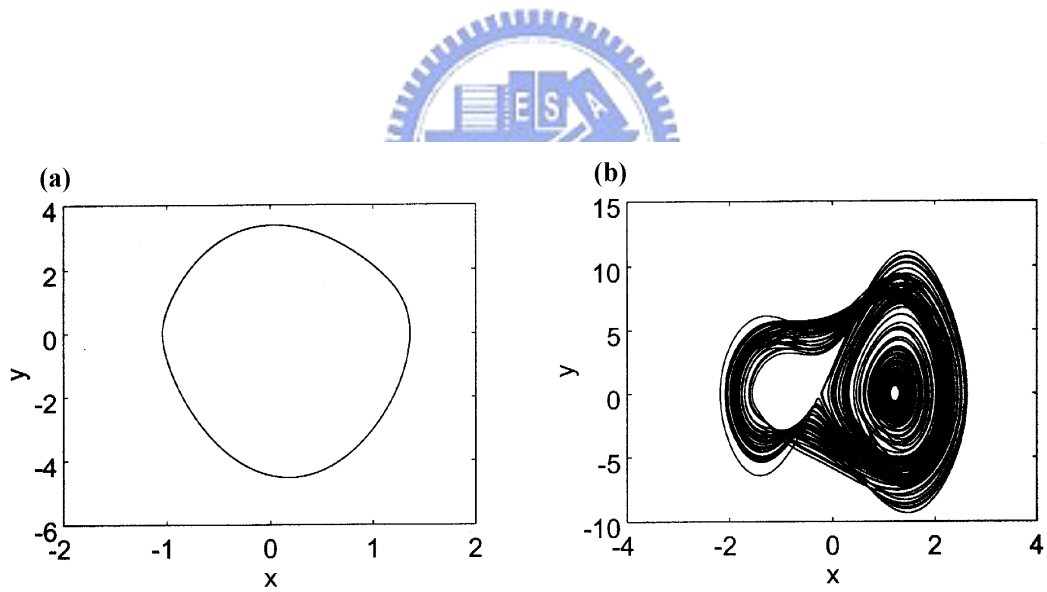
Fig. 3.25. (a) Phase portrait for $q=3$ (b) $q=5.5$
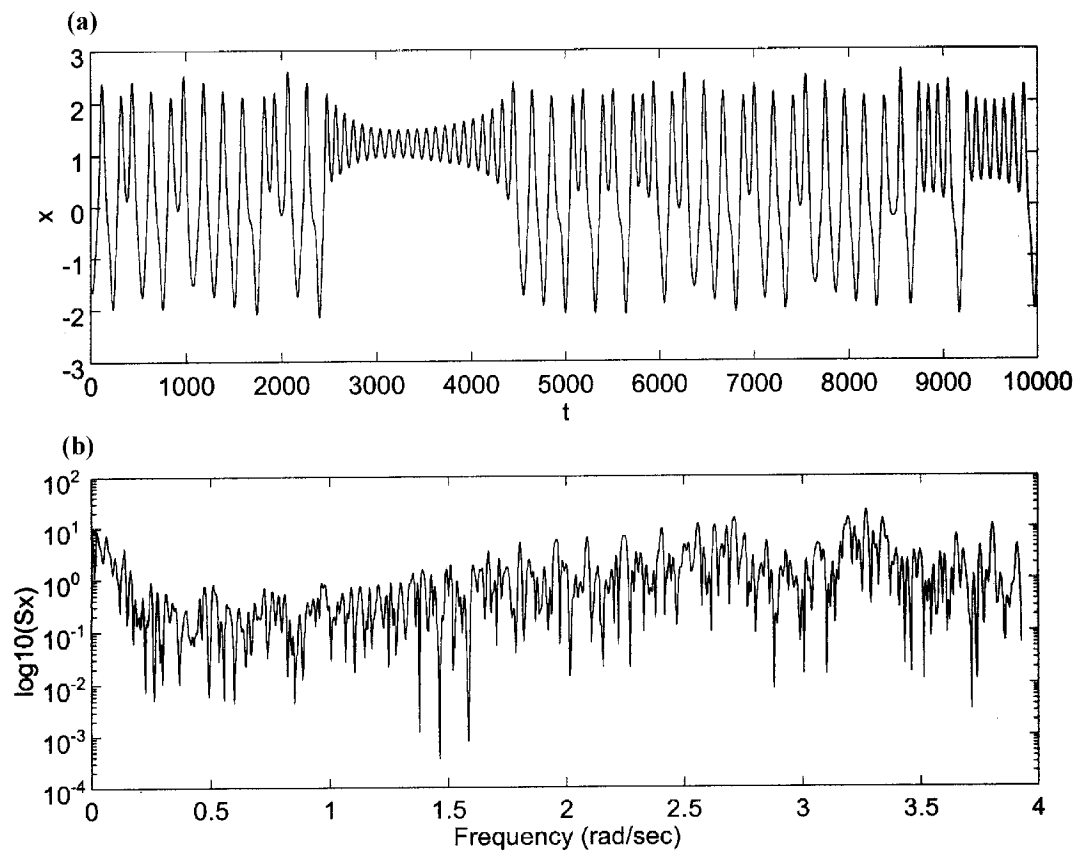
Fig. 3.26. (a) Time history ,(b) power spectrum for q=5.5
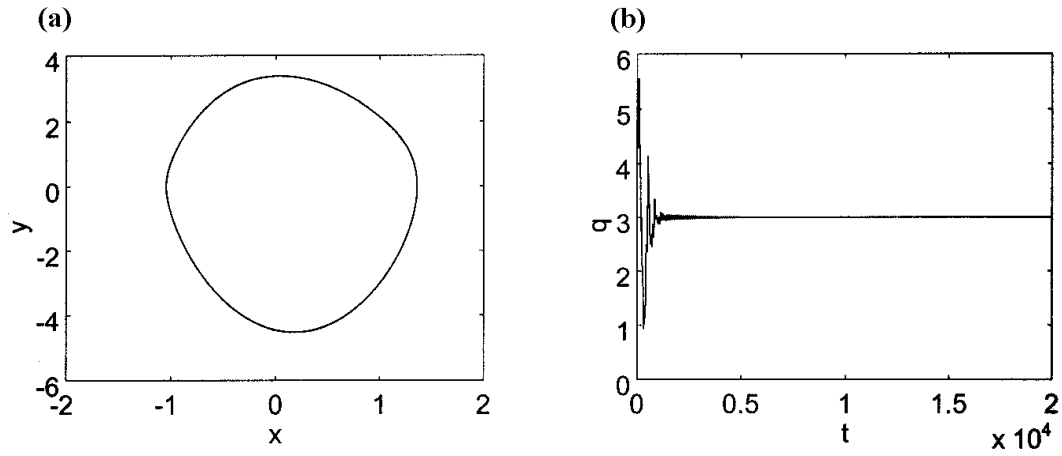
Fig. 3.27. Controlled system via adaptive feedback.
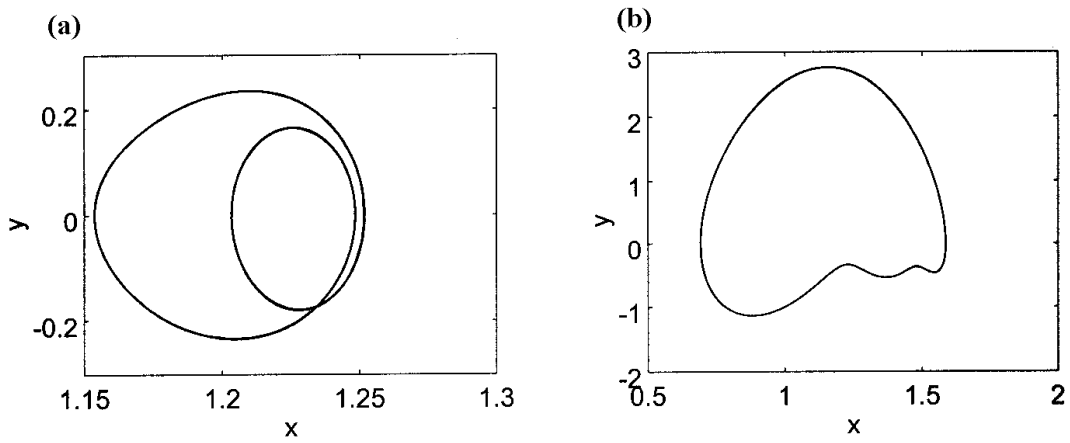
Fig. 3.28. (a)Phase portrait of controlled system via linear feedback control for $K_2 =$
0.5,   (b) $K_2 = 5$
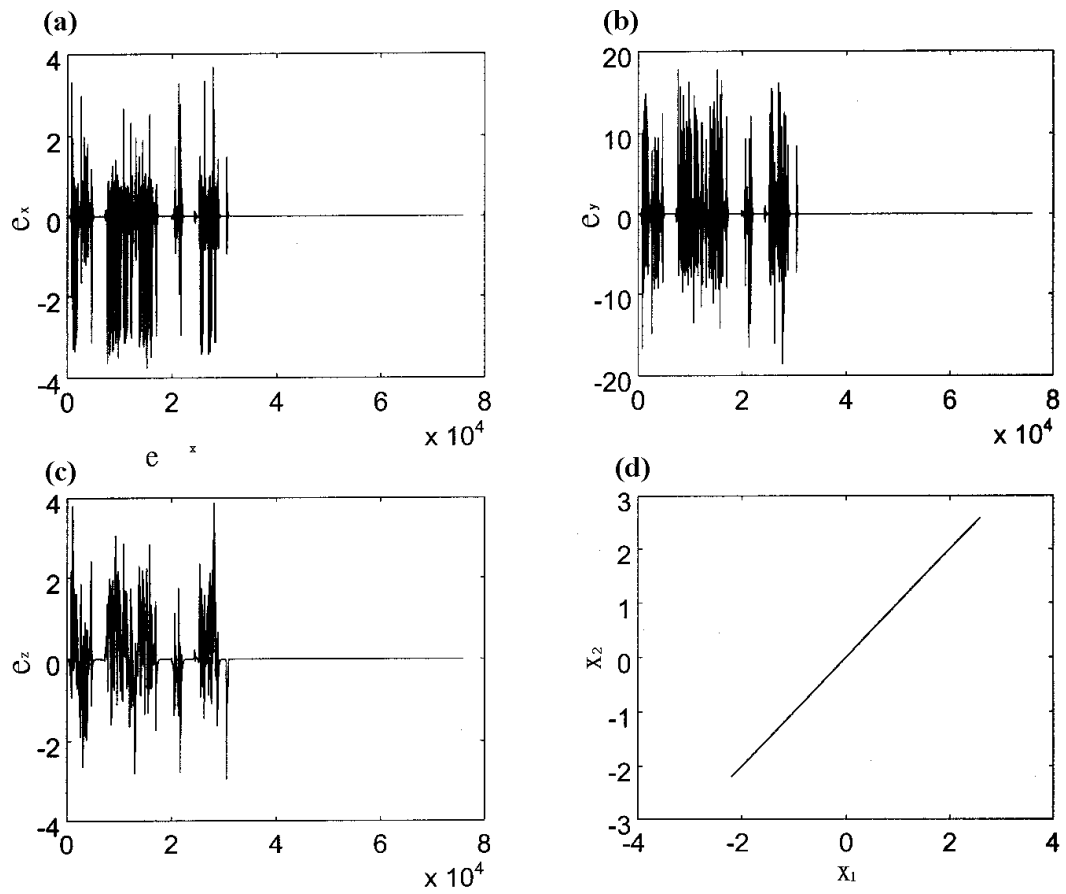
Fig. 3.29. Chaos synchronization via a unidirectional linear feedback approach for K=3.
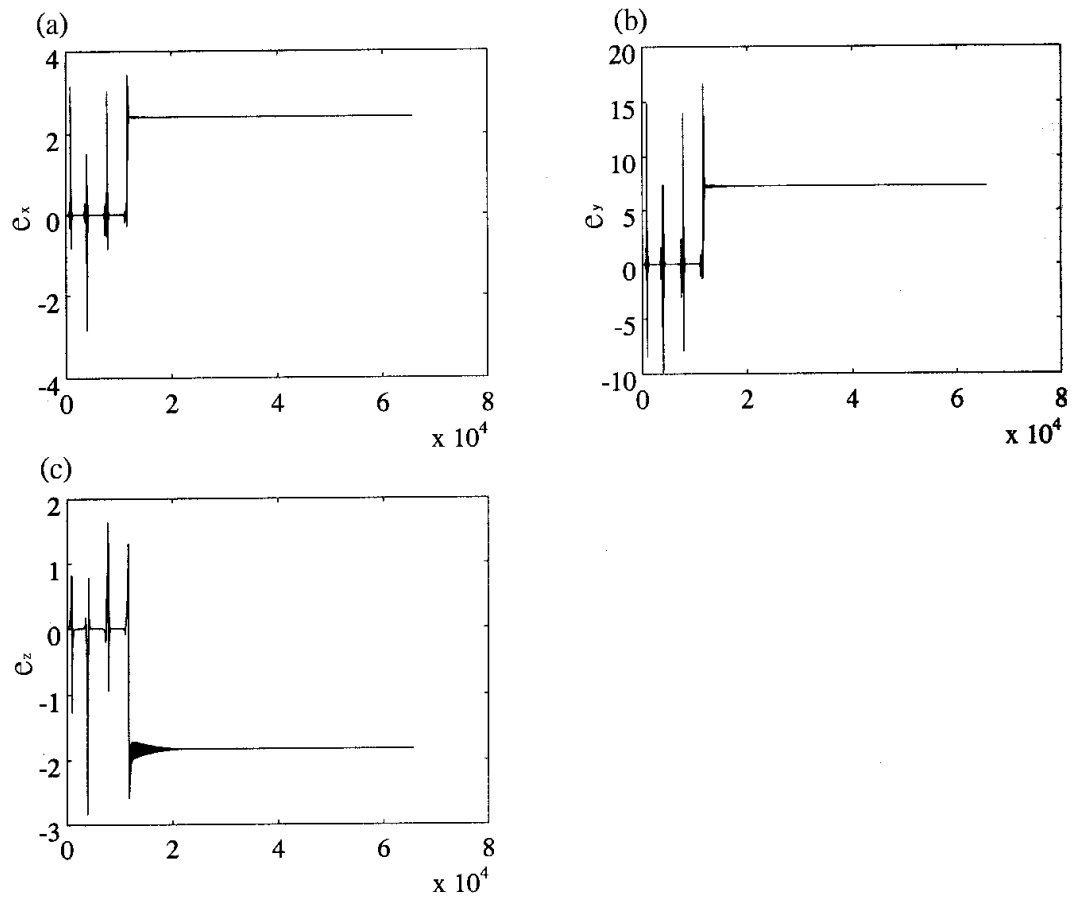
Fig. 3.30. Chaos synchronization via a mutual linear feedback approach for K=1.5.
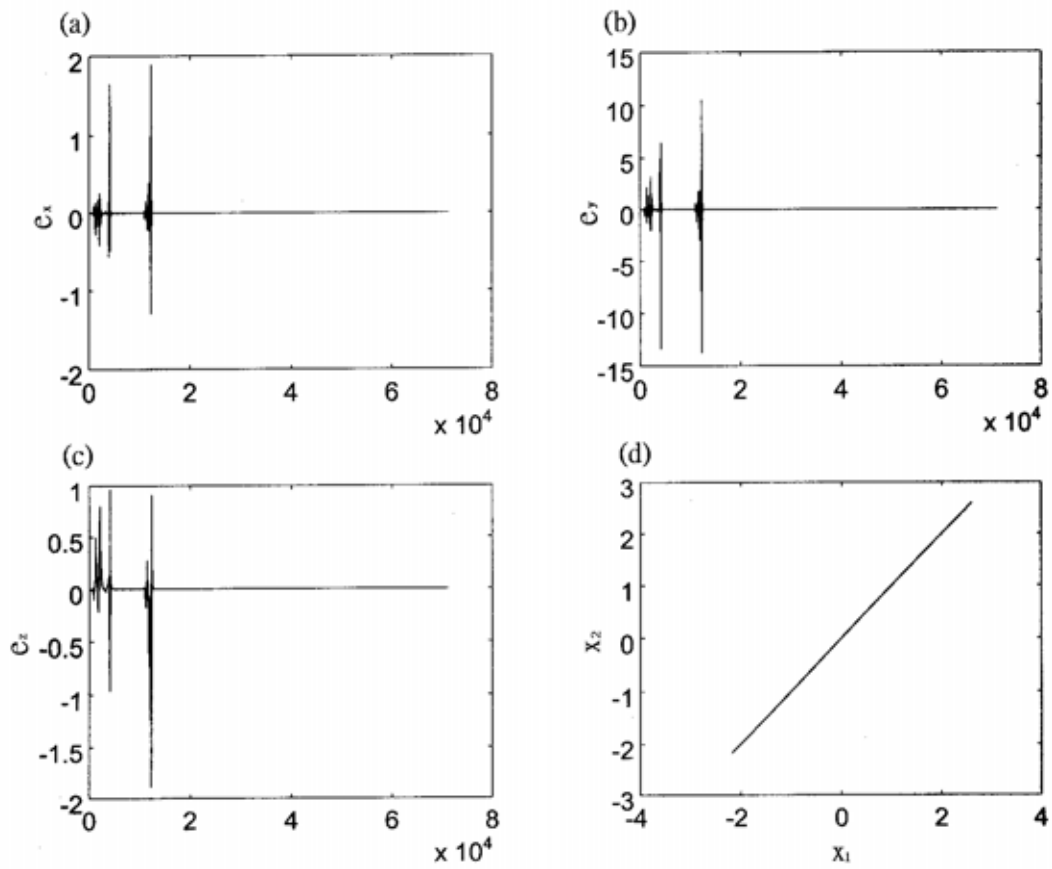
Fig. 3.31. Chaos synchronization via a mutual linear feedback approach for K=3.
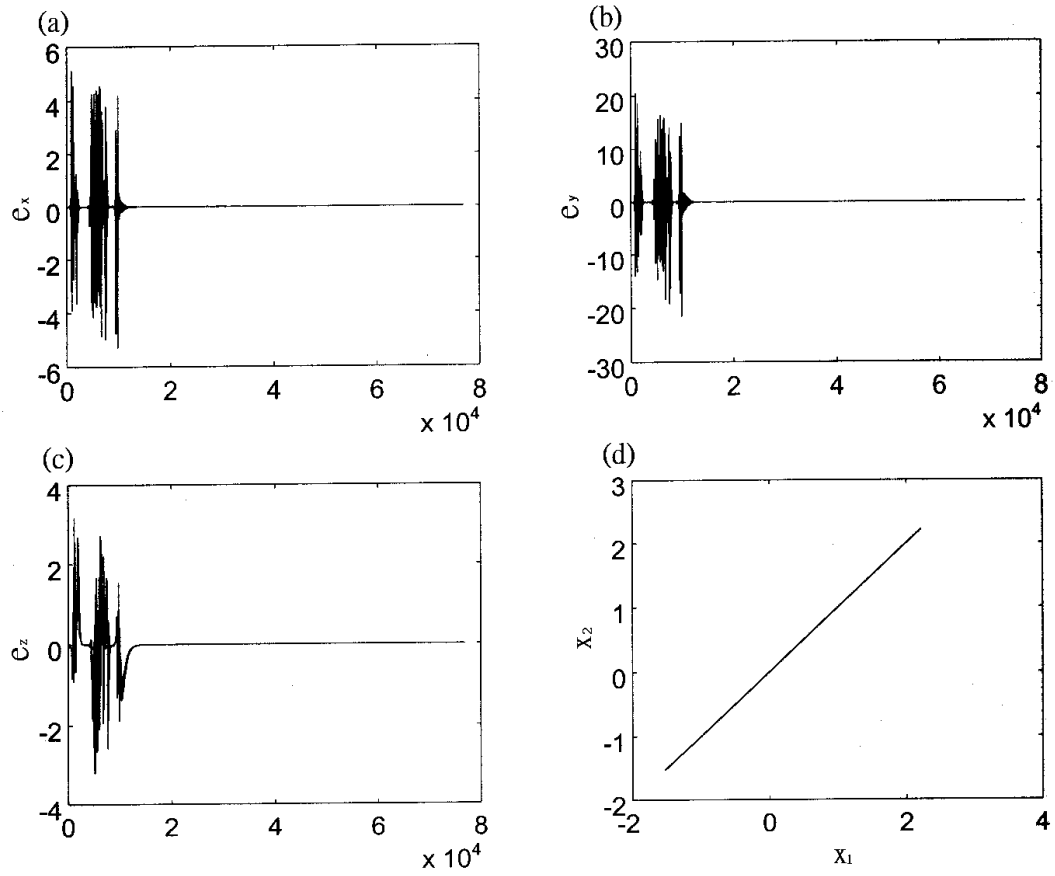
Fig. 3.32. Chaos synchronization via a mutual nonlinear feedback approach for K=1.5.
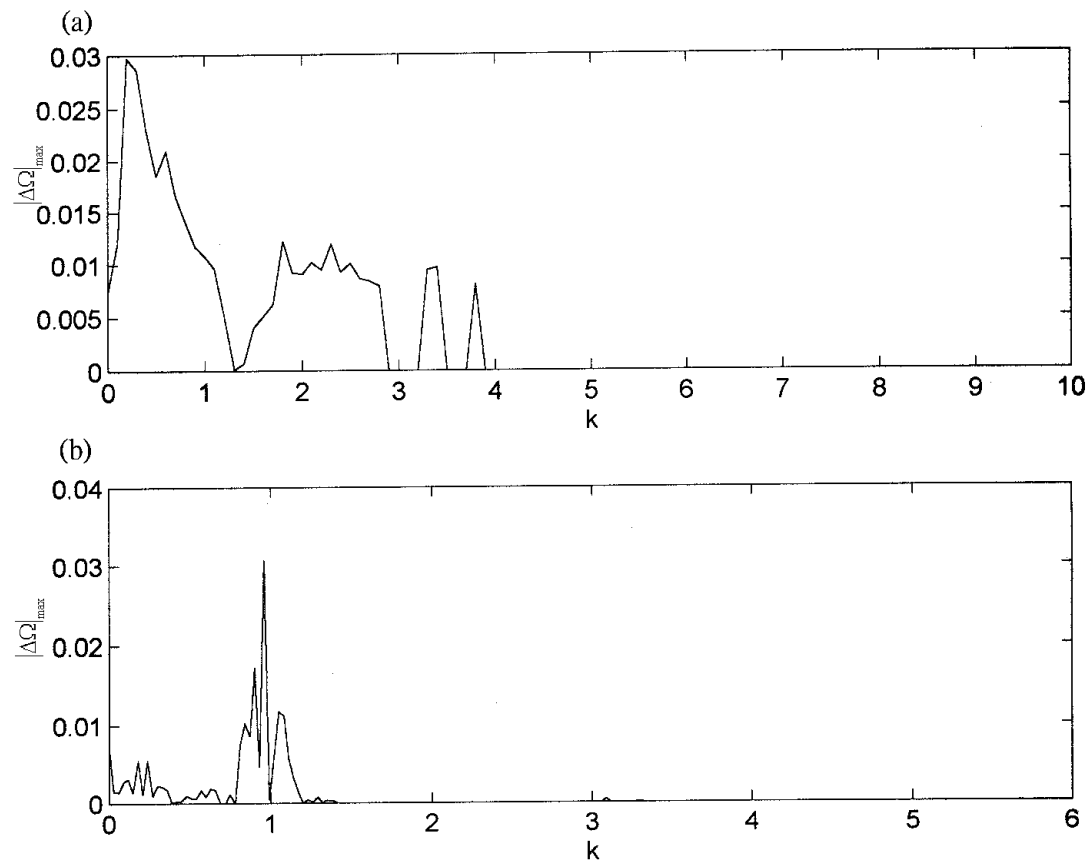
Fig. 3.33. The maximum absolute difference of mean frequency between two chaotic subsystems.
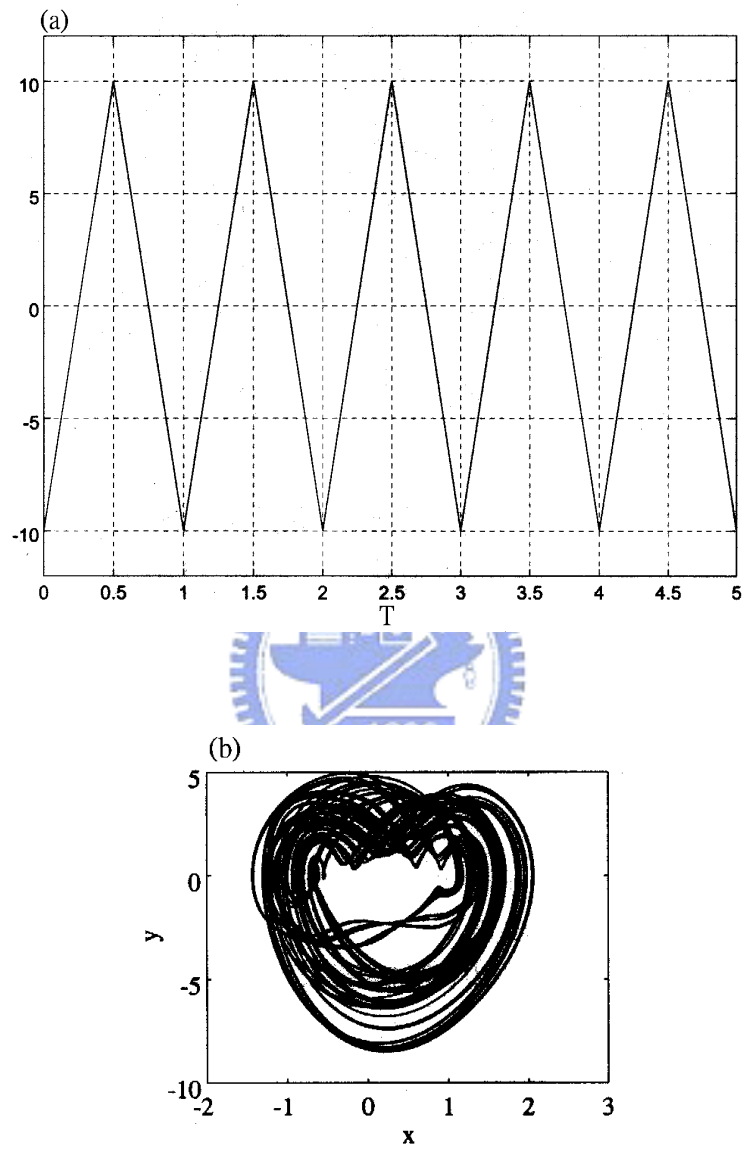
Fig. 3.34. (a) A sawtooth function, (b) Phase portrait of controlled system.
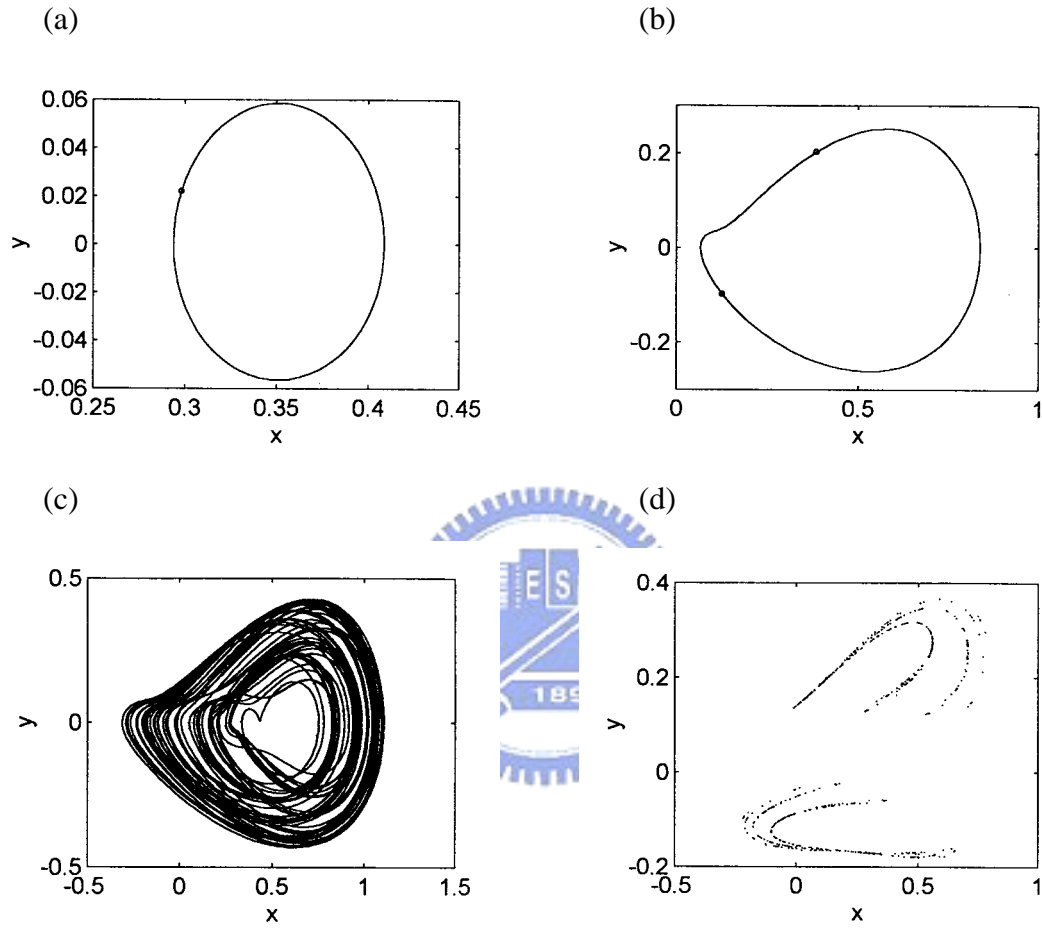
Fig. 3.35 (a) Phase portrait and Poincaré map for *q*=2.07 (b) *q*=2.14 (c) phase portrait for *q*=2.21 (d) Poincaré map for *q*=2.21

(a)

(b)
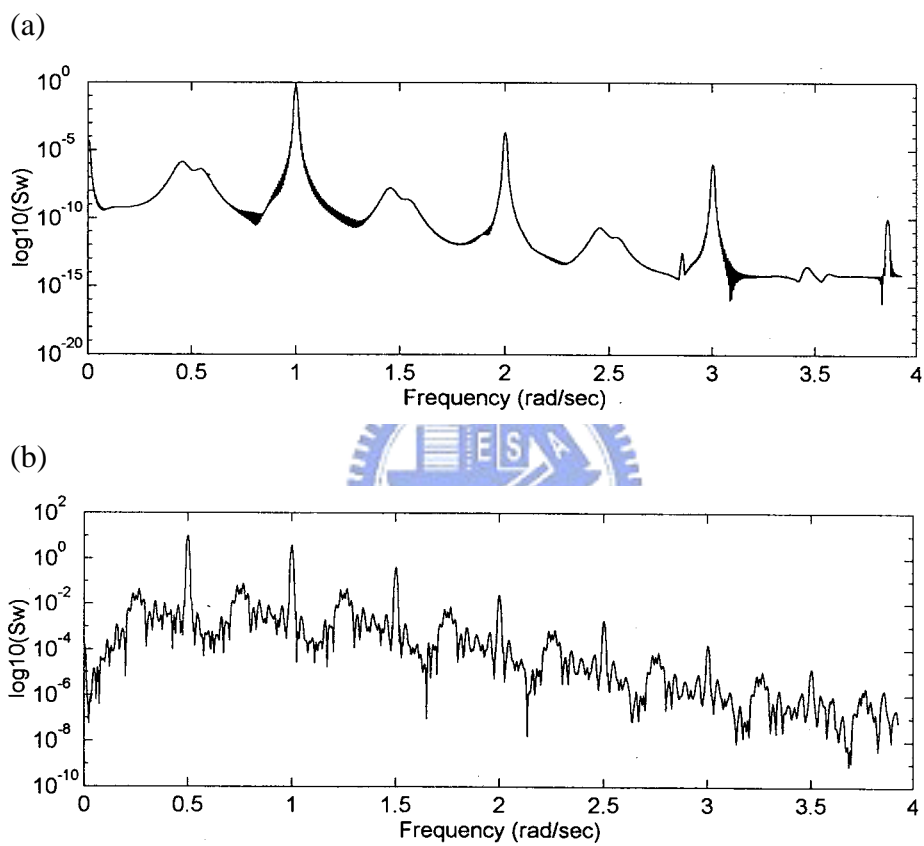
Fig. 3.36 (a) Power spectrum for q=2.07 (b) q=2.21

84
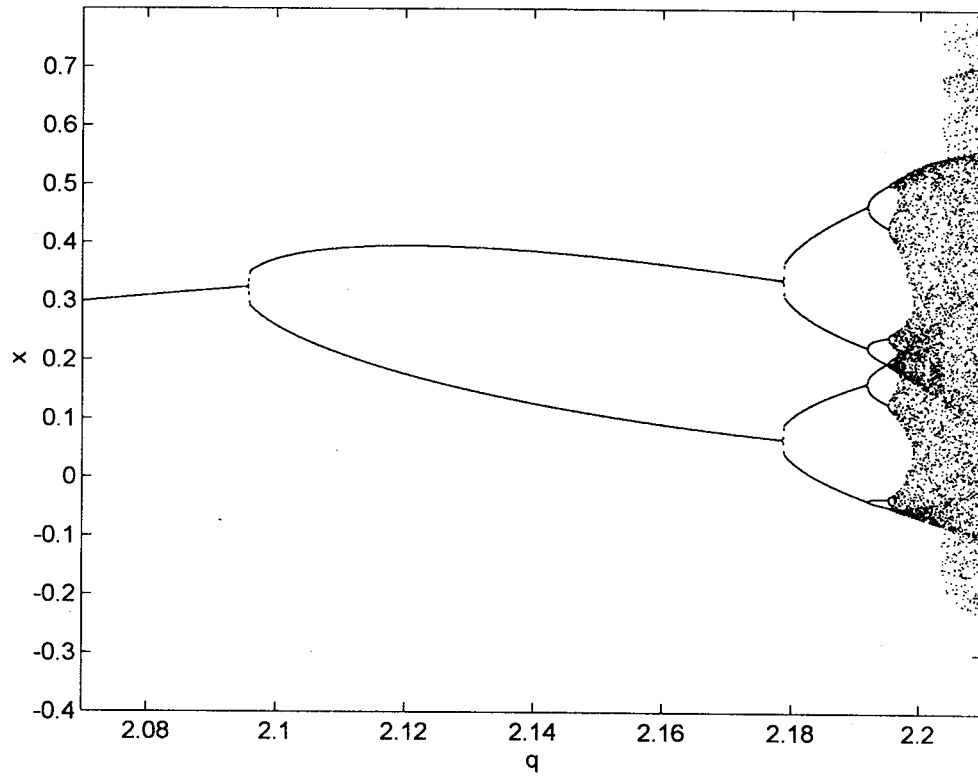
Fig. 3.37 Bifurcation diagram of q versus x

(a)
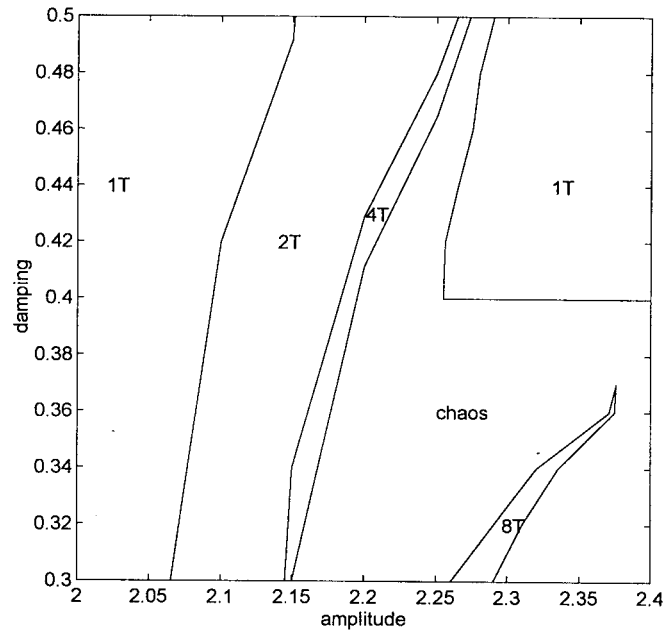
(b)
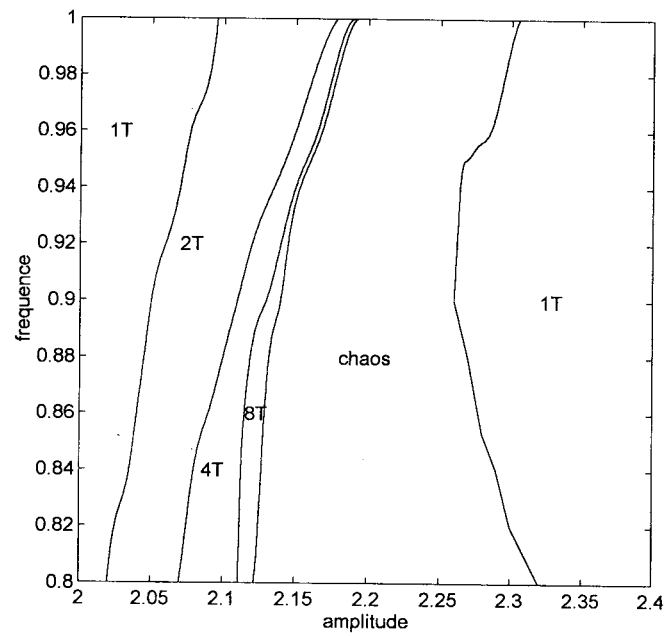
Fig. 3.38 (a) Parametric diagram of q versus b (b) q versus $\bar{\omega}$

86
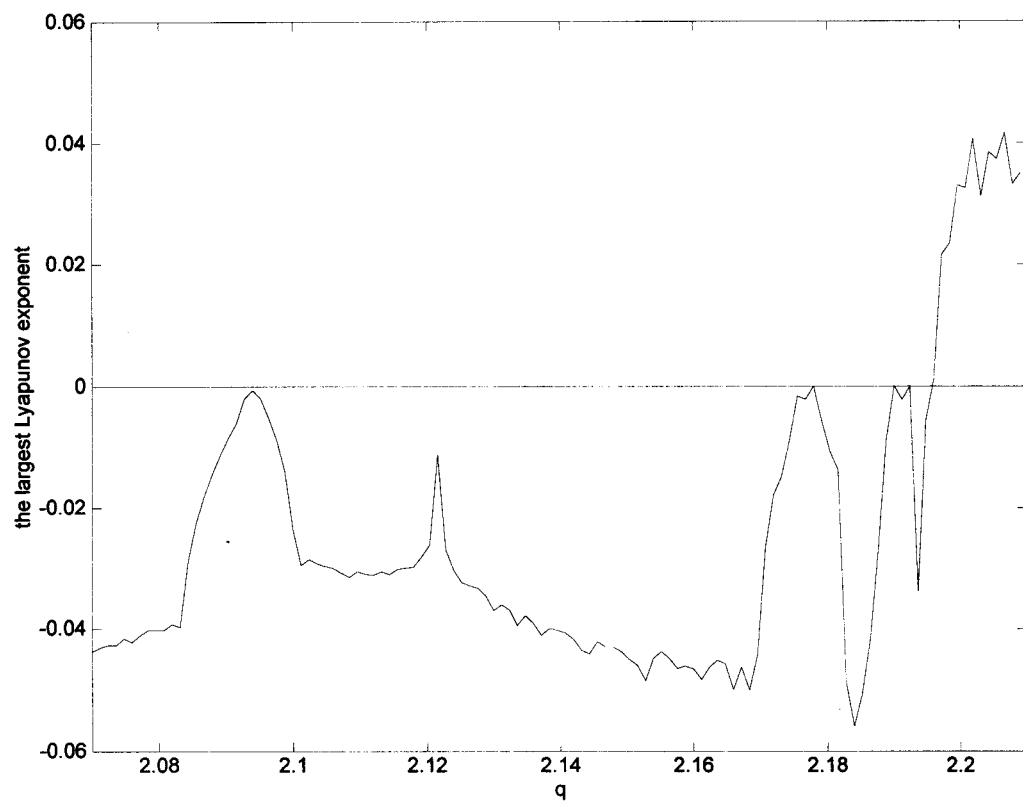
Fig. 3.39. The largest Lyapunov exponent for q between 2.07 and 2.21
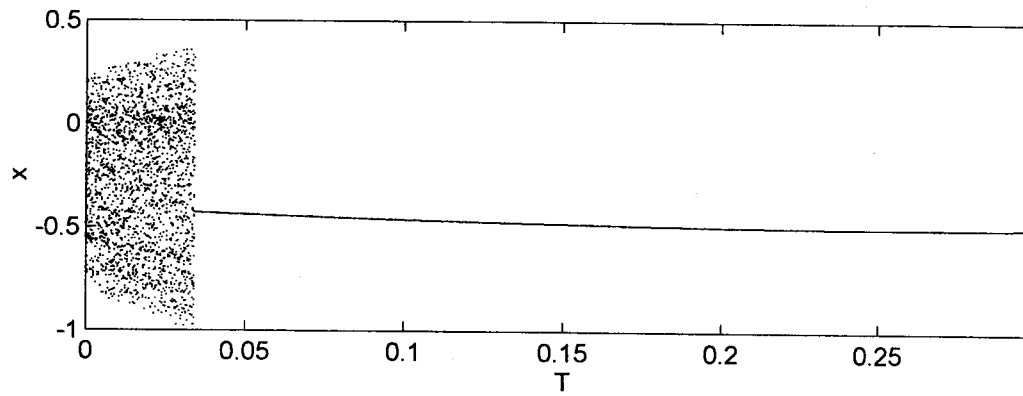
Fig. 3.40. Bifurcation diagram of T versus x
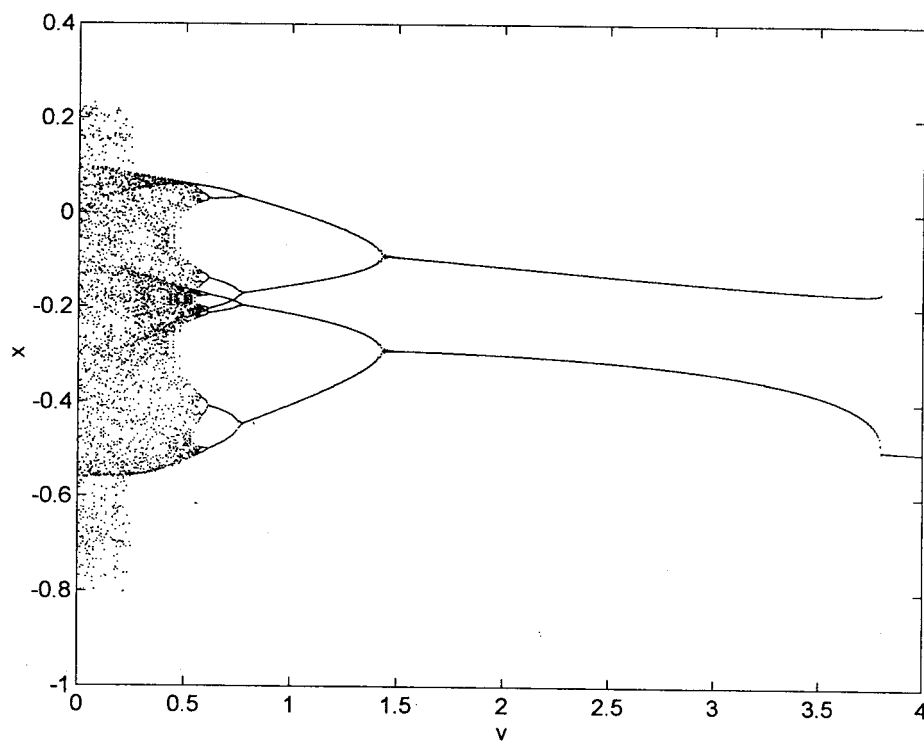
Fig. 3.41. Bifurcation diagram of v versus x

88
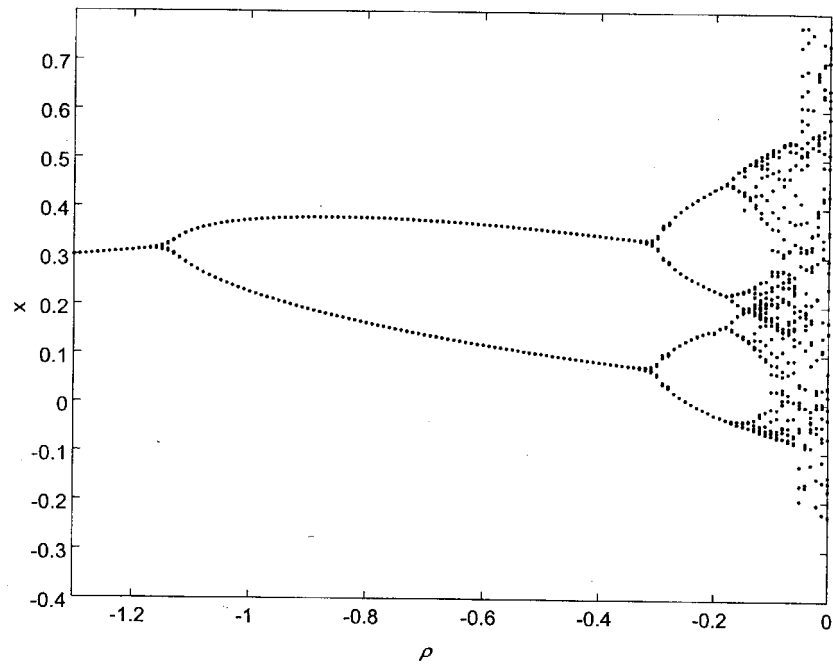
Fig. 3.42. Bifurcation diagram of ρ versus x
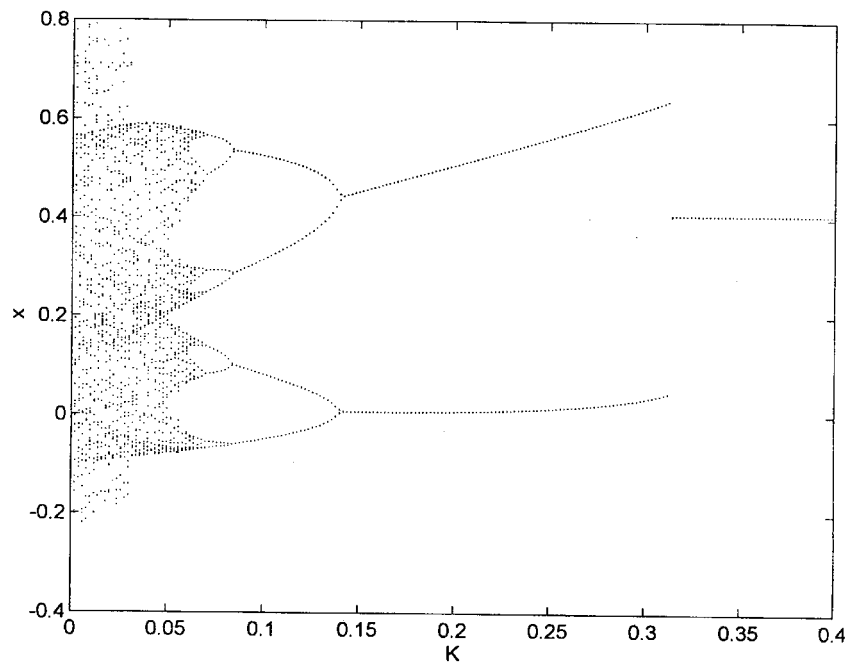
Fig. 3.43. Bifurcation diagram of K versus x
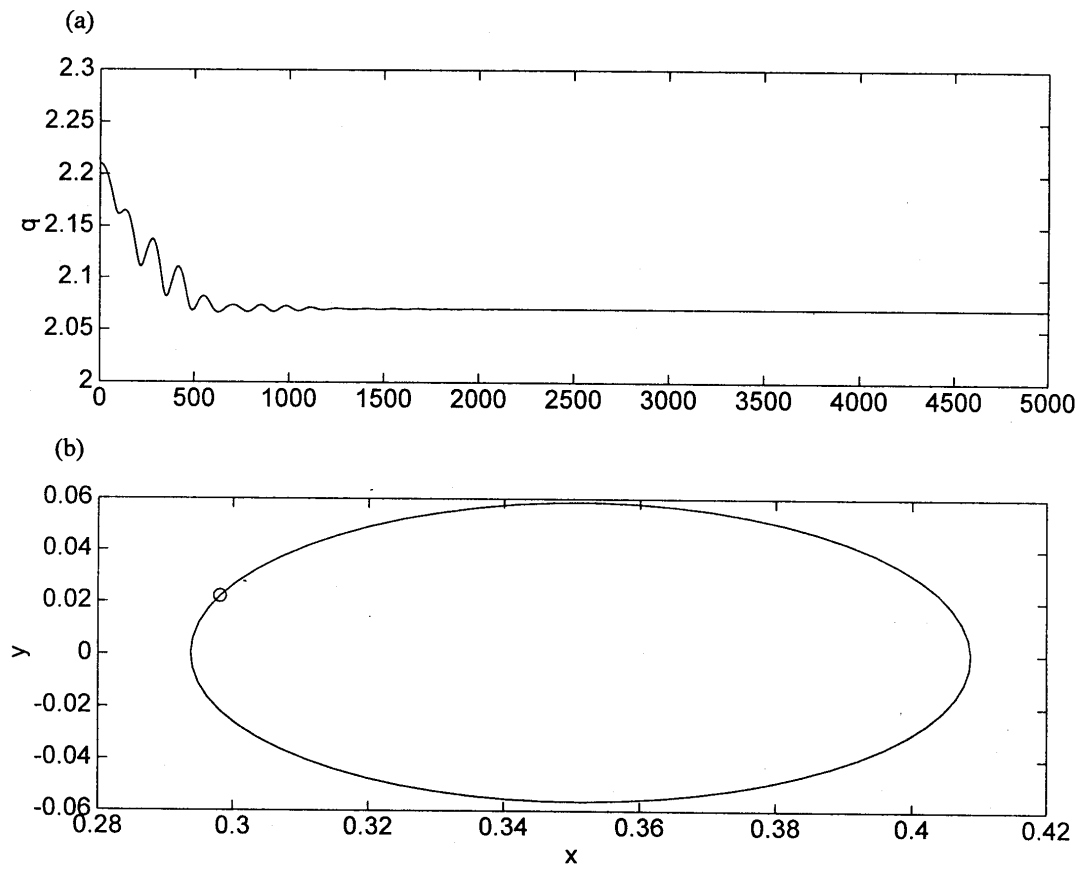
Fig. 3.44. (a) Parameter converge to q=2.07 from chaotic motion q=2.21 (b) Phase portrait and Poincaré map of controlled system
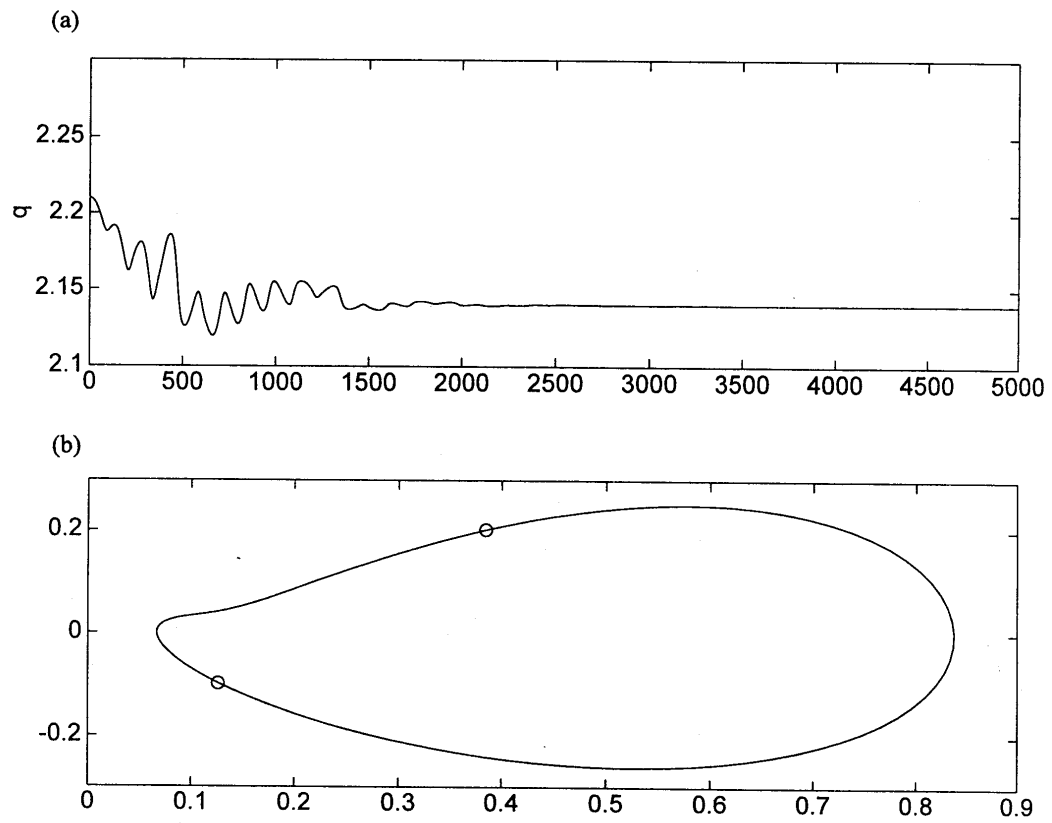
Fig. 3.45 (a) Parameter converge to *q*=2.14 from chaotic motion *q*=2.21 (b) Phase portrait and Poincaré map of controlled system
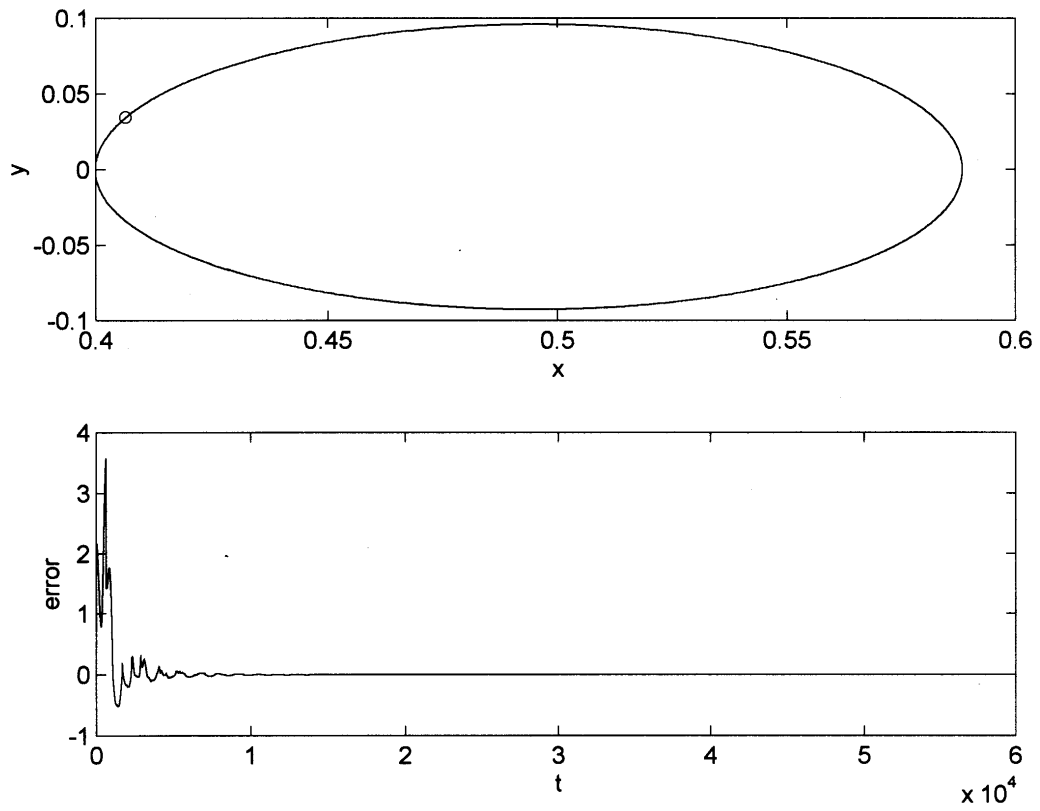
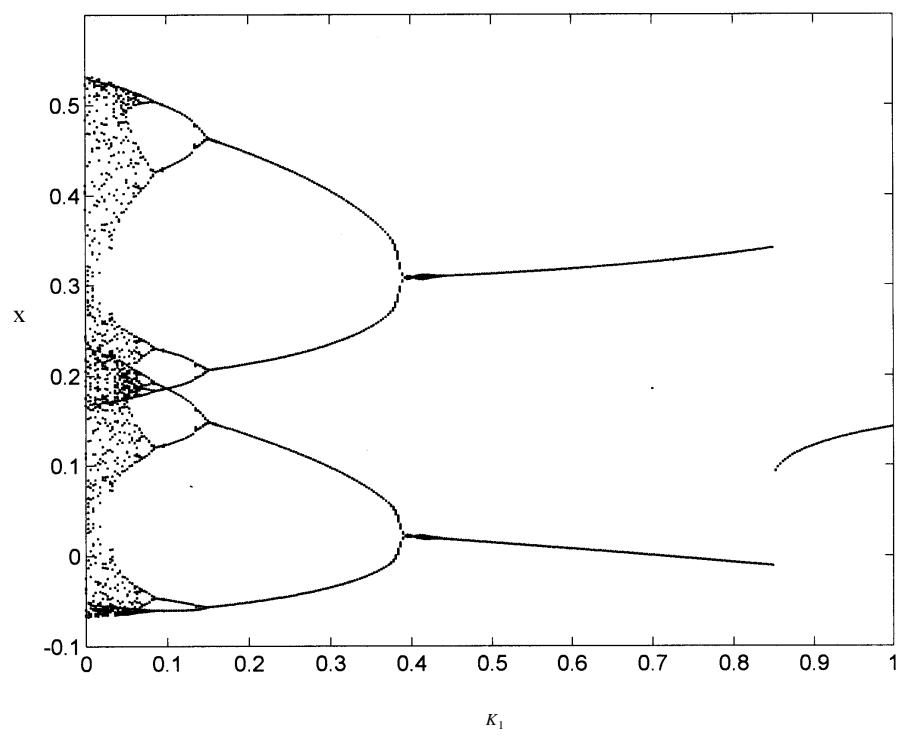Fig. 3.46 (a) Phase portrait and Poincaré map of controlled system (b) the error signal

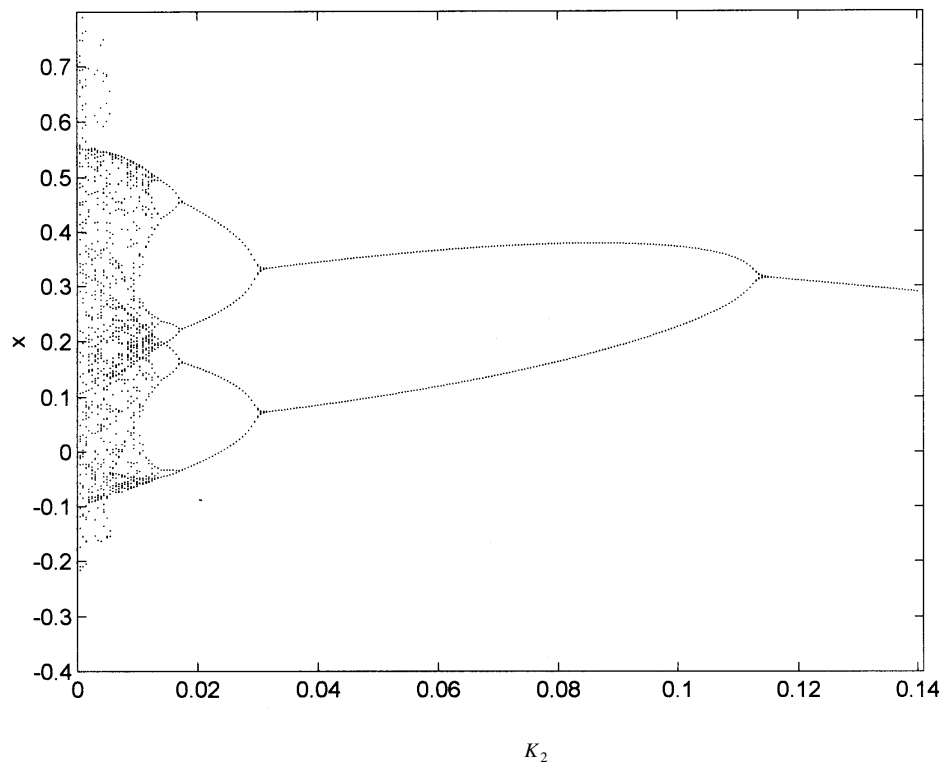Fig. 3.47. Bifurcation diagram of K_1 versus x

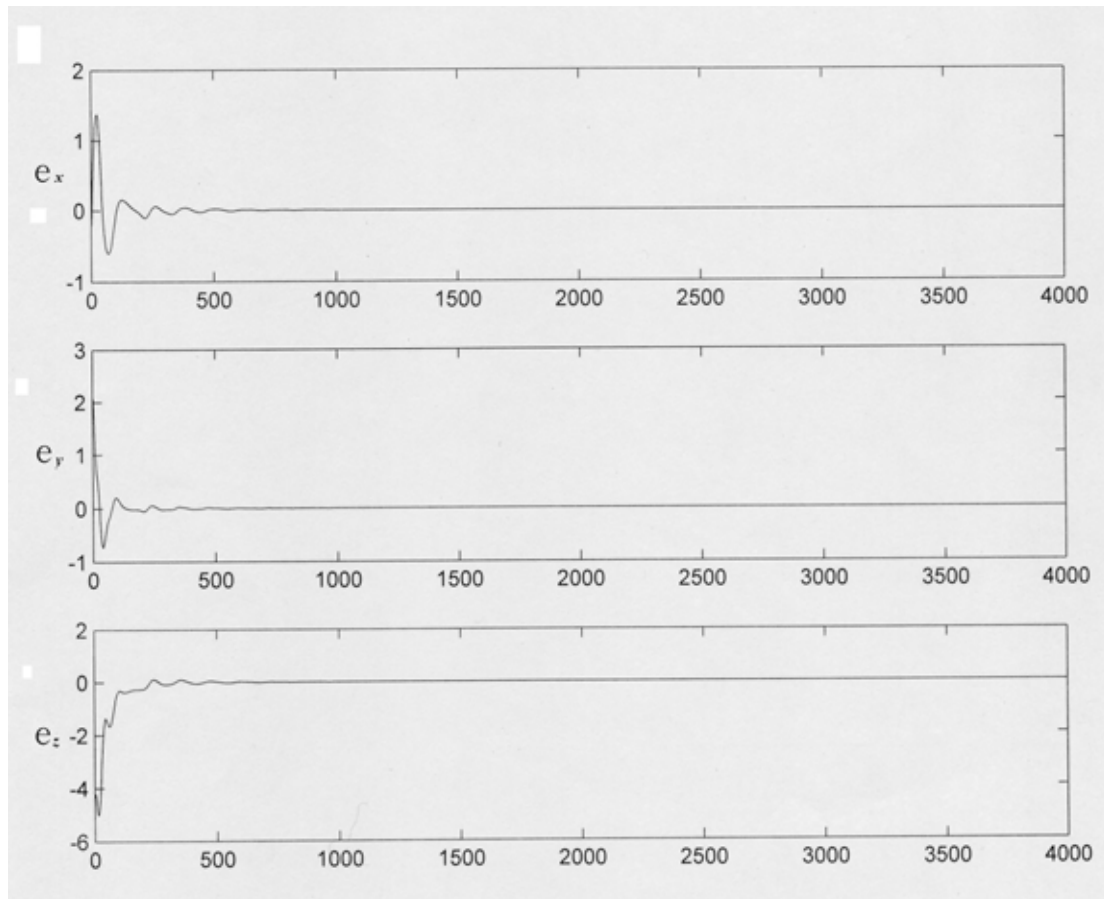Fig. 3.48. Bifurcation diagram of K_2 versus x

Fig. 3.49. Chaos synchronization via linear feedback with k =0.2.